Concepts NREC

The Experts in Turbomachinery

TECHNICAL MEMORANDUM NO. 1817
Concepts NREC Project No. 10614
Prepared for: Diffuser Consortium Phase VI Sponsors

Project Director: David Japikse
Project Manager: Sharon E. Wight
By: David Japikse, Sharon E. Wight, Jamin J. Bitter, Mark R. Anderson, Ali Mahallati, Andrew R. Provo, and David M. Karon

April 10, 2015

ADVANCED CENTRIFUGAL PUMP AND COMPRESSOR CONSORTIUM
FOR DIFFUSER & VOLUTE DESIGN, PHASE VI

PROGRESS WITH THE INTERNATIONAL DIFFUSER CONSORTIUM, Abridged Version

TECHNICAL MEMORANDUM NO. 1817

PROGRESS WITH THE INTERNATIONAL DIFFUSER CONSORTIUM

TABLE OF CONTENTS

TABLES

FIGURES

TECHNICAL MEMORANDUM NO. 1817
Concepts NREC Project No. 10614
Prepared for: Diffuser Consortium Phase VI Sponsors
Project Director: David Japikse
Project Manager: Sharon E. Wight
By: David Japikse, Sharon E. Wight, Jamin J. Bitter, Mark R. Anderson,
Ali Mahallati, Andrew R. Provo, and David M. Karon
April 10, 2015

ADVANCED CENTRIFUGAL PUMP AND COMPRESSOR CONSORTIUM
FOR DIFFUSER & VOLUTE DESIGN, PHASE VI

PROGRESS WITH THE INTERNATIONAL DIFFUSER CONSORTIUM (Abridged Version)

ABSTRACT

Phase VI work on the Diffuser Consortium is nearing its end. Essential trends of the 1990s investigations have been confirmed and clarified with detailed data now available to validate design methods and to establish fresh insights to the basic flow processes of the pr = 3.5, Ns = 110 stage. Several fundamental departures from historical perceptions have been identified, including: the flow field naturally develops circumferential variations (confirmed independently), work may be done or total temperature variations may exist in front of the impeller due to rotating blade pressure fields, and the velocity triangles at impeller exit can be forcibly changed by using the newly patented flow-wise grooved cover. Special studies on surge line movement and diffuser inlet pinch have been made. Balanced pinch and rear pinch (alone) are better than front pinch, which is the industrial default design at this point. Continued work is recommended, including critical laser velocimeter measurements of the impeller exit and diffuser inlet region with and without flow-wise cover grooves, and also including other stages.

1.0 INTRODUCTION

Phase VI Diffuser Consortium investigations have focused on developing a deeper understanding of the best diffuser designs as tested in the 1990s and the physics behind the performance. More comprehensive instrumentation was used for the front, rear, and double pinch vaneless diffusers, as well as two high-performing LSA diffusers, and the flat-plate and the double divergence diffusers (including comprehensive full flow field traversing, right up to the stability limit). These formed a core set of high technology diffusers worthy of deeper investigation. It was clearly recognized at the outset that rotor – stator interactions were significant and needed detailed study. A strong desire existed to modify this interaction to bring benefits to the design process.

Work started with a comprehensive review of the past five (5) investigations. Some new insights were garnered, and a specific list of preferred stages for continued detailed investigation was created. A core focus throughout all this work was to extend operating range and improve stage efficiency, also with the hope of eventually increasing diffuser pressure recovery on the order of 80% for vaned diffusers. CFD was used extensively to investigate key performance issues and to develop a more complete understanding of the detailed flow field, beyond that which could be confirmed by measurements. Validation of the CFD tools was also undertaken. The balloting process gave useful guidance midway through the work, when the

traversing goal for the double or balanced pinch vaneless diffuser was switched to the front pinch configuration, in order to give a more complete data picture (this change was the strongest voting decision of the group). Voting also gave some input for extra work in the second year as more sponsors joined the process.

The end results of this work were satisfying. All studied geometries have a more detailed data picture, and many have a better CFD understanding. Strong evidence not only of coupling but also easily measured flow field distortion was revealed that begs deep questions about periodicity. This area of thinking led to the invention of the flow-wise-grooved covers with very nice range extension and increased work input. This procedure should allow one to tailor preferred velocity profiles in the future.

The Phase VI work (see Appendix 1 for Statement of Work) is a restart of the efforts of the 1990s and began in the area of greatest question and opportunity using the highest Ns impeller. The entire prior work, however, actually used three different impellers covering a very wide application base, as shown here in Figure 1. Various sponsors and potential sponsors have asked for increased attention to some of the other flow regimes, which should be at the heart of continued work.

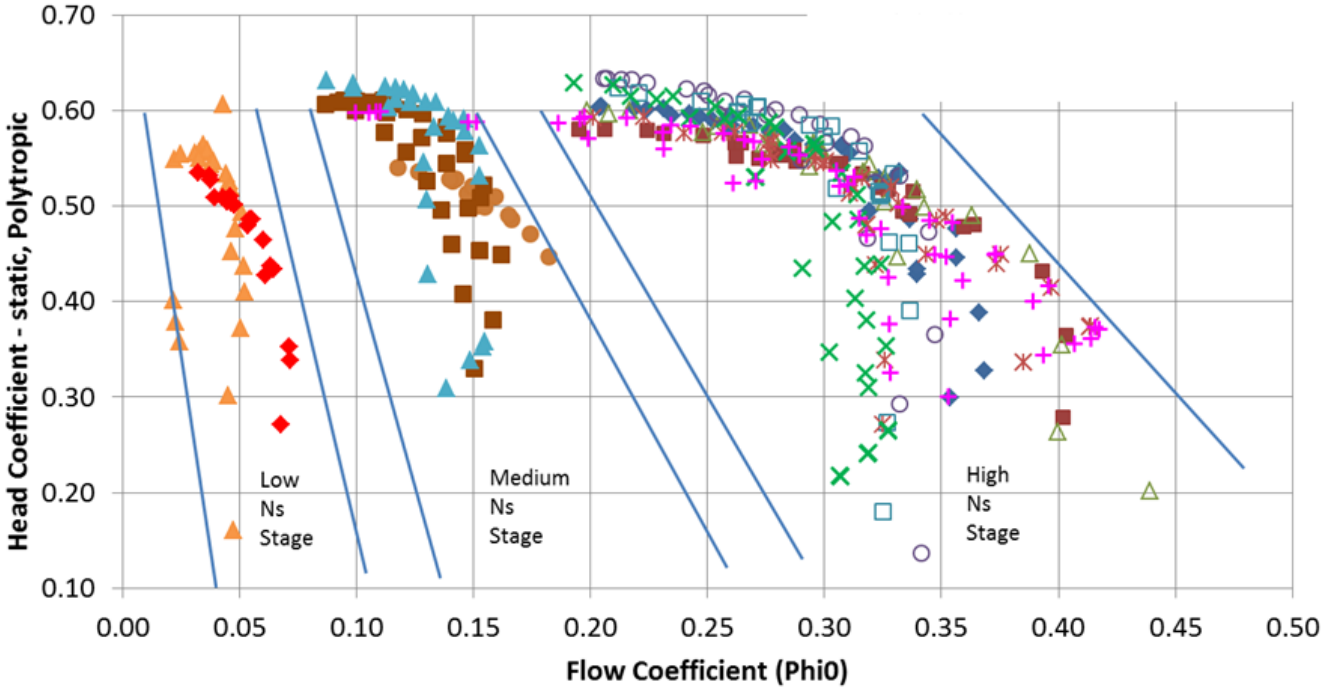

Figure 1. Flow regimes for the past diffuser consortium investigations using all classes of diffusers and three different impellers and test rigs

2.0 EVALUATION OF 1990s DATA

The data and insights acquired in the 1990s were based on three stages, indicated in Figure 1. For the first three phases, the 60 mm test rig was employed, followed by two more stages for Phases IV and V.

2.1 Past Test Hardware and Results, Phases I - III

Figure 2 shows the first test rig, and it used a common turbocharger impeller and cover plus bearing housing for all of the first tests. With time, the rough quality of the cast impeller was improved, as shown in Figure 3, by first using a well cleaned-up cast impeller, and then (for current work) using a precision-machined impeller. The turbine was replaced with a

mixed-flow turbine, so that the turbine inlet temperature could be drastically reduced and matched to the same value as the compressor discharge temperature, in order to eliminate heat transfer between the compressor and the turbine. The rigs are thoroughly insulated as well.

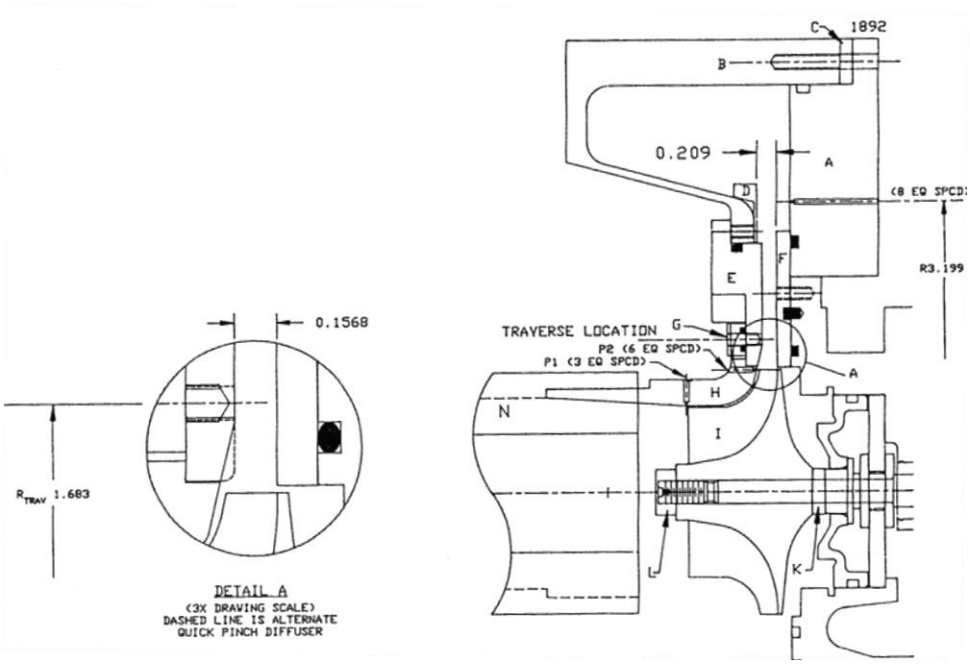

Figure 2. The 60 mm test rig with a front pinch vaneless diffuser, the 16 bladed turbocharger Ns = 110 pr = 3.5 impeller, and the inlet duct A long inlet duct is necessary to gain access for traversing.

Figure 3. Evolution of the Ns = 110 test stage; the final configuration is precision-machined

This test rig has been used for three decades and has produced much quality data; details are given in Appendix 2. For the 1990s work, inlet and exit pressures, temperatures, and flow were measured, plus impeller exit static pressure on the front surface, and of course speed was measured. Full flow field traversing was conducted at one location just downstream of the impeller exit. Operating clearances were controlled at 0.009 inch by translating the cover to be centered around the axis of operation. (Prior to the middle of Phase II, the eye clearance was several times greater due to the usage of an OEM cover and looser bearings.) All testing since has tight clearance control.) More details are available in Appendix 3.

Some of the key data obtained in this facility include the following examples:

2.1.1 Example 1

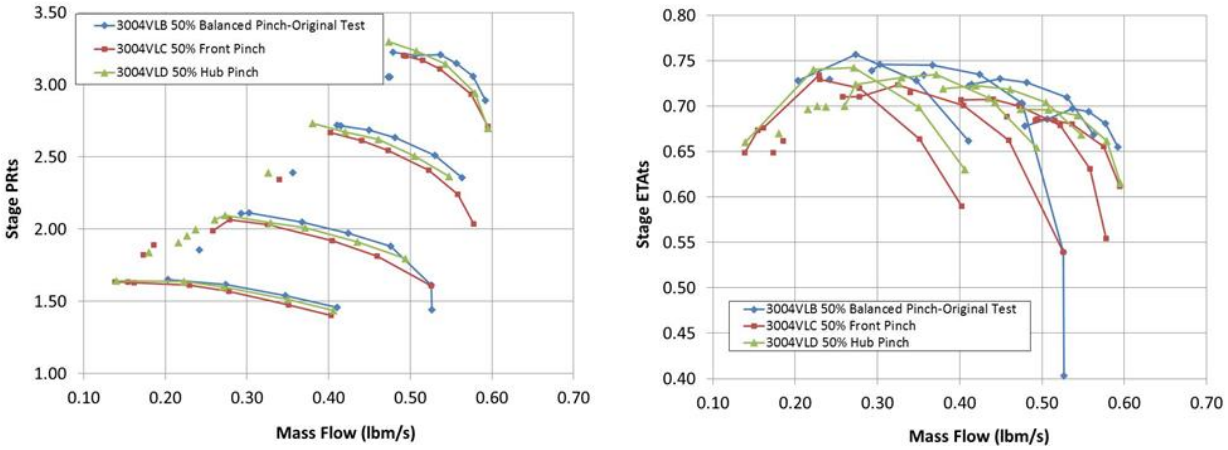

Figure 4. 50% pinch vaneless diffuser; the balanced pinch shows highest pressure ratio and efficiency, followed by the rear pinch, while the front pinch has the lowest values

All three cases in Figure 4 have the exact same one-dimensional (1D) velocity triangles and the same area distribution throughout. The balanced pinch gives the highest head rise and efficiency at all speeds. The rear pinch case gives the widest range and the best rise to surge, but its efficiency is about 1 or 2 points lower than the balanced pinch. The front pinch case is the lowest of all three on all counts. Similar results were found with only 25% pinch.

2.1.2 Example 2

For the 25% pinch, a comparison can be seen, as shown in Figure 5.

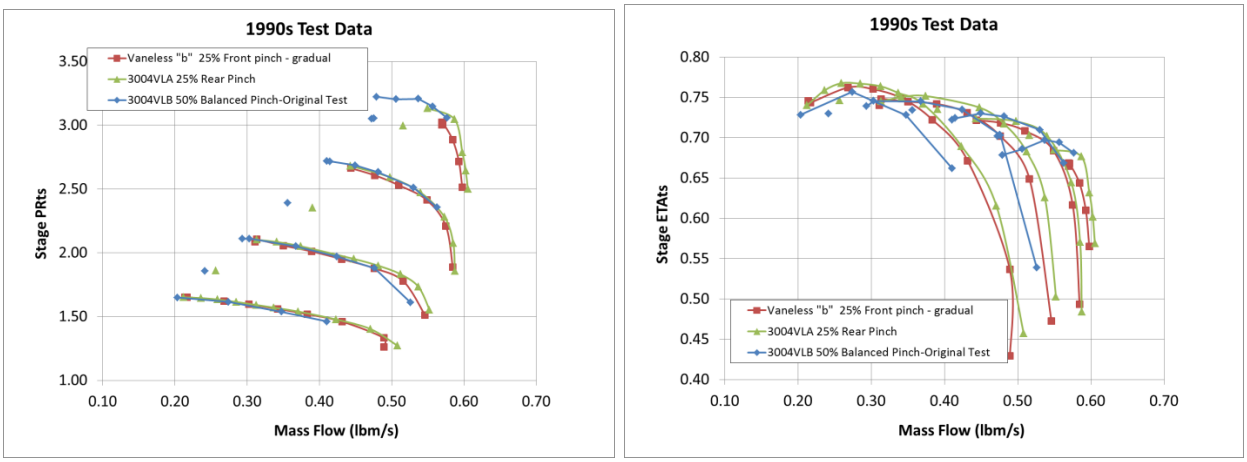

Figure 5. Comparison of 25% front and rear pinch vaneless diffusers with 50% pinch, ca. 1990s

From the Figure 5 results, one can conclude again that it is better to have rear pinch than front pinch, and 50% performs much better than 25% except for efficiency at lower speeds and pressures. Reasons for this are not totally clear, but new insight has been gained in the current work. The 50% balance pinch case essentially extends the trends of the 25% pinch case to lower flows, but does not lift the 25% pinch pressure rise at the same flow rates; it does however lose 1 – 3 points of efficiency at low speeds.

2.1.3 Example 3

Detailed studies of various vaned diffusers were also made, and key cases are summarized here.

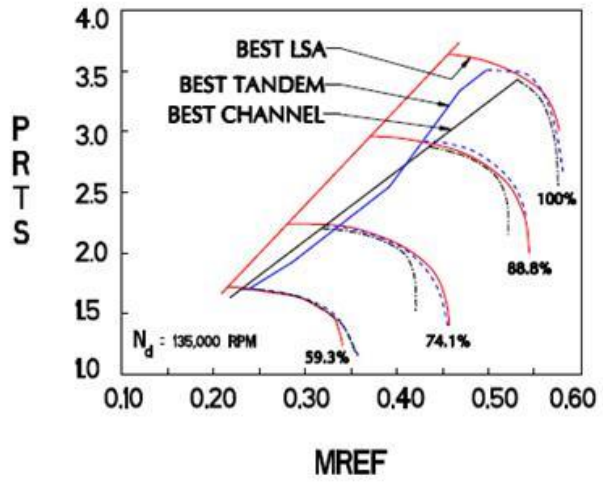

Figure 6. Key vaned diffuser results

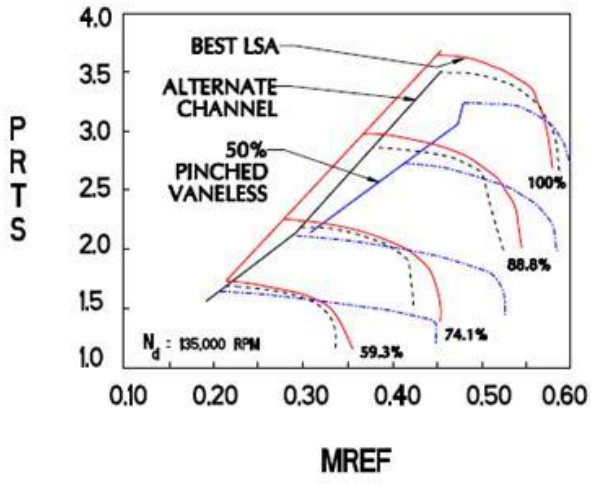

Figure 7. Other key diffusers, plus the 50% pinched vaneless

The cases shown in Figures 6 and 7 illustrate the wide range and the high efficiency of the LSA diffuser. The channel diffuser also performed well, but not quite on par with the LSA. When this was shown in the early 1990s, some LSAs were already in production, but this work opened many doors for many companies, as the LSA rightfully became recognized as a top performing diffuser. It is also clear that for pr > 2.5, the LSA has better stable operating range than does the vaneless diffuser unless it is severely pinched, but then it will lose more efficiency.

Two more important cases need mentioning from the 1990s work, and these are the flat-plate diffuser (an LSA variant) and the double divergence channel diffuser. Figures 8 and 9 illustrate these two cases.

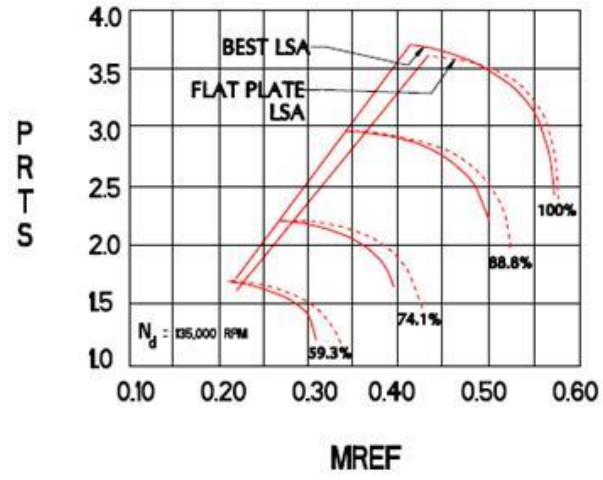

Figure 8. Comparison of the flat-plate LSA variant with the best LSA; essentially the same pressure, range, and efficiency has been achieved with this simple flat-plate configuration

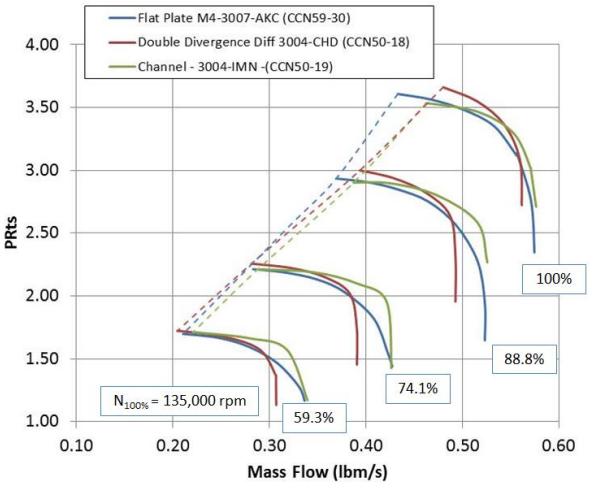

Figure 9. The double divergent diffuser compared with a wide-range channel diffuser and the flat-plate LSA diffuser

These select cases illustrate the important variances, and some surprise configurations, that were established in the 1990s. These cases inspire considerable opportunity for further invention and product development.

2.2 Past Test Hardware and Results, Phases IV & V

Two additional test rigs and stages of lower specific speed were introduced in Phases IV and V. The low Ns = 55 stage had a maximum pressure ratio of pr = 1.8 and was characteristic of industrial barrel pumps and compressors, blowers, and many single-stage pumps. The medium specific speed compressor at Ns = 85 had pr = 4.5 and was typical of some gear-driven compressors, various gas turbine compressors, and ship and locomotive turbocharger compressors. The first of these two has been extensively tested with many different vaneless diffuser configurations and at variable Reynolds number; however, only a small portion of this work was done specifically for the Diffuser Consortium. Most of this work was done for a related Stability Consortium, and all of this work will be brought together during the next phase of this consortium. The Phase IV work did include both vaneless and LSA diffuser research. The medium pressure ratio stage has been tested with LSA, simple channel, and conical diffusers. This last stage is a good candidate for the flow-wise grooved cover and also to check double divergence and flat-plate diffuser designs. A few examples are included in the cases given below.

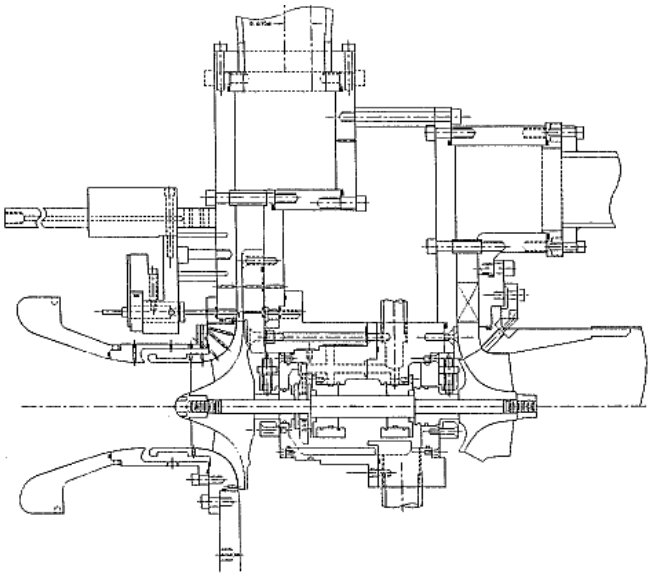

Figure 2.93. The 90 mm rig used in the medium specific speed testing.

Figure 10. The Ns = 85, pr = 4.5 rig with a vaneless diffuser and a traverse setup

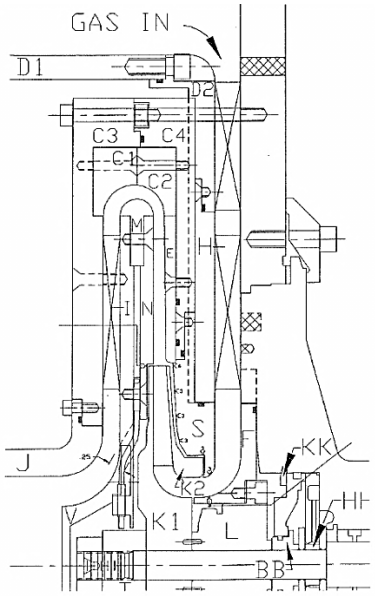

Figure 3.2. Cross section of the low specific speed test rig.

Figure 11. The pr = 1.8, Ns = 55 test rig with an unpinched vaneless diffuser and a return channel element

The test rigs used for these important alternatives are fully available and will likely be put back into operation for Phase VII. The Figure 10 rig is our 90 mm rig, whereas the Figure 11 rig is our 120 mm rig. Very precise measurements have been made on each, and detailed traverses have also been conducted. During Phase VII work, it is expected that the related work for the Stability Consortium (now available on the consortium secure data site) will be integrated with the Diffuser Consortium work, giving a very detailed study of industrial process compressors and the onset of rotating stall.

2.2.1 Example 4

Select results for the low Ns case are partially shown in Figures 12a, 12b, and 12c. In this case, the LSA has been used to extend stable operating range. Both the vaneless and the LSA are viable types for this application, as is the flat-plate diffuser. The latter should be added to this study, along with investigations of the grooved cover.

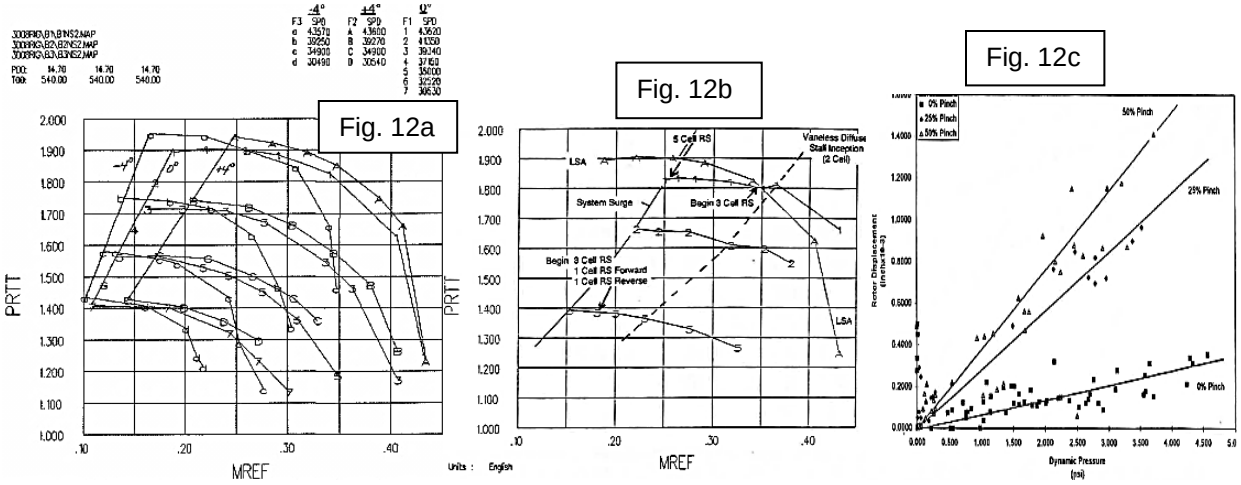

Figure 12a. Low Ns stage with LSA; Figure 12b. One of many vaneless map tests showing greater range with the LSA; and Figure 12c. Shaft displacement with stall cell dynamic pressure as a function of diffuser pinch for rotating stall in the vaneless diffuser

2.2.2 Example 5

The pr = 4.5 stage (Figs. 13 – 15) is a true transonic stage and gives all the challenges of the highly loaded stages. Three types of diffusers worked well (the vaneless also was tested, but it is noncompetitive, above pr = 2.5). Nonetheless, the conical diffuser seems to hold special merit, and hence, this rig is already in a rebuild state being readied for additional tests.

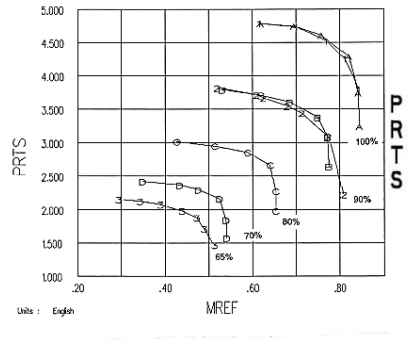

Figure 13. Results from the Ns = 85, pr = 4.5 stage; best LSA and best channel

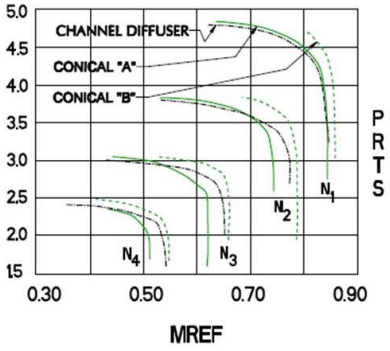

Figure 14. Stage performance with the conical diffuser

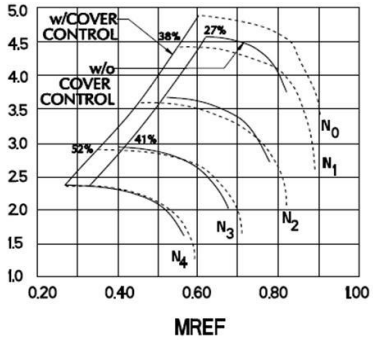

Figure 15. With cover bleed for range extension

Range extension for many applications has often been necessary for higher Ns stages, and the pr = 4.5 stage shows the same ability for extension as many others of its class (see Figure 16).

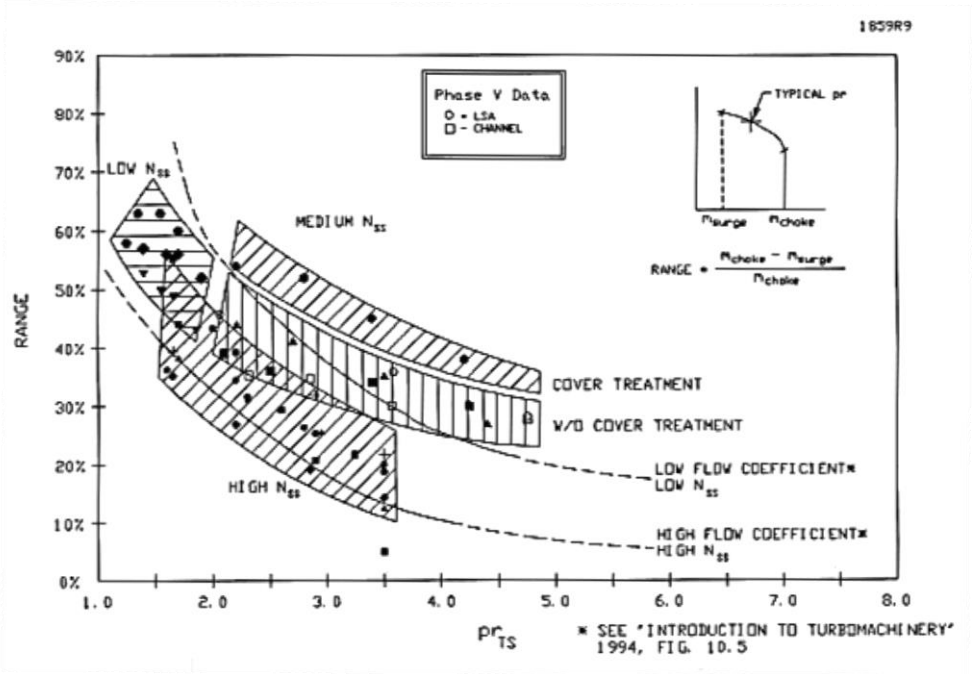

Figure 16. Increase in stable operating range with the cover bleed

2.2.3 Example 6

A study has been initiated of the firmness of the surge lines for various stages. For the 60 mm rig, a fairly tight band is seen for the vane-type diffusers, and the best stages always show surge well to the left of the vaneless diffusers.

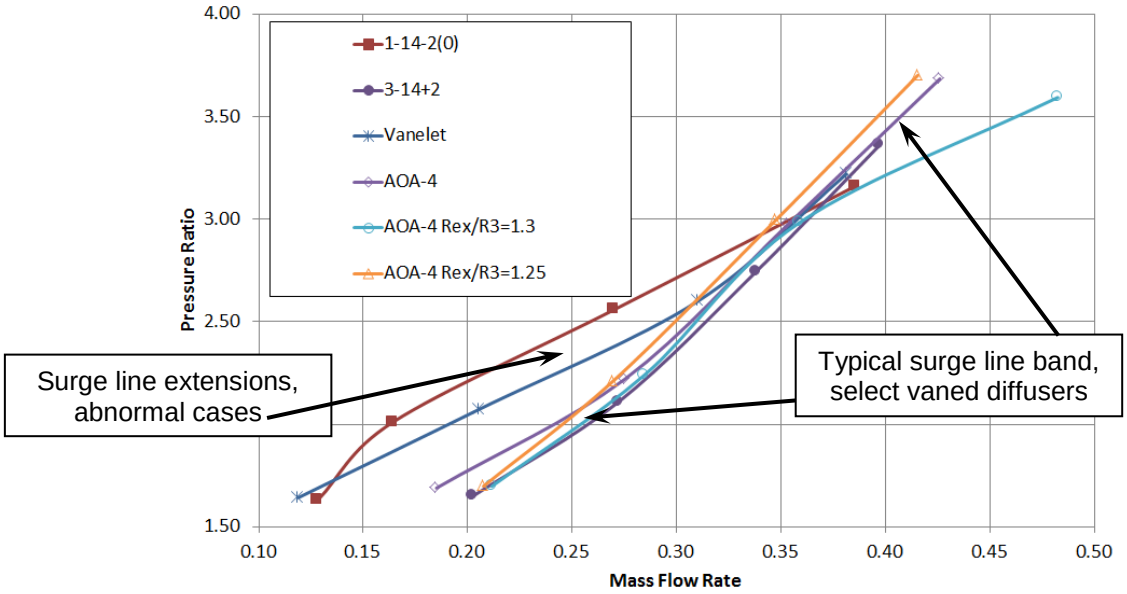

Figure 17. Lowest surge lines for various Ns = 110 tests with both channel and LSA diffusers

It may be seen in Figure 17 that a band of four good vaned-type diffusers have essentially the same surge line. Two other cases show more stability at low pressures; these two cases are not regular diffusers and would not be a marketable entity; still, they raise the point that lower flow rates can be achieved by *some* means.

Figure 18 shows the Phase V results of looking at the pressure field between two vanes, with a channel diffuser shown on the left and an LSA on the right (Fig. 19). Significant vane-to-vane distortion seems to be evident; later, these data will be reinterpreted on a circumferential basis (see Appendix 7), where confirmation of actual circumferential variations is given.

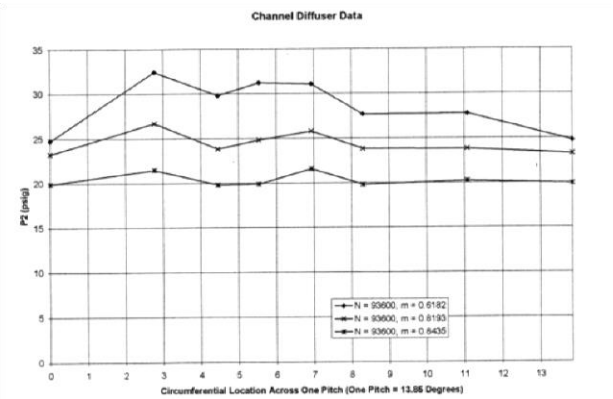

Figure 18. Perceived vane-to-vane pressure variation for the Ns = 85, pr = 4.5 channel diffuser

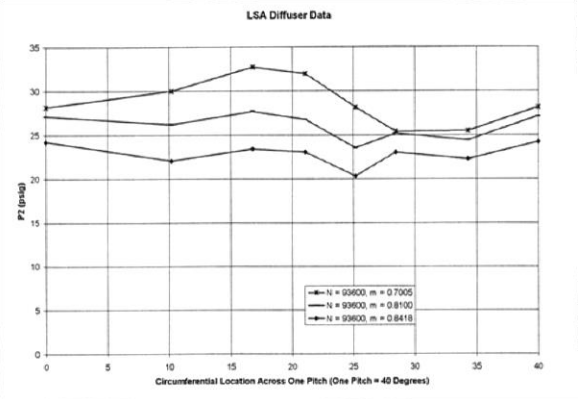

Figure 19. The same for an LSA diffuser

2.3 Past Results and CFD, Phases I - V

The use of the Reynolds-averaged Navier-Stokes (RANS) equations, and solutions thereof, which is commonly called CFD or Computational Fluid Dynamics, was employed in the 1990s for guidance in that earlier consortium work. Solutions for all three stages were obtained.

Since the Ns = 110 stage was an accepted industrial stage, CFD was used only to study the trends and explore internal flow states a bit better. For the Ns = 85 and Ns = 55 stages, CFD was used to guide the actual design process, and various design alternatives were examined, with the best case selected for construction. In the early 1990s, CFD was used mostly as a design tool, and only limited off-design analysis was pursued. At that time, validation of CFD codes was in an early stage of pursuit.

TABLE I. A COMPARISON OF ANALYTICAL AND EXPERIMENTAL CHANGES DUE TO COUPLING EFFECTS

	CFD		TEST DATA	
	UNCOUPLED	COUPLED	UNCOUPLED	COUPLED
P_{OO}, PA	101300	101300	101353	101353
P_2, PA	224140	234392	273777	280366
% Increase in P_2	Base	+4.6%	Base	+2.4%
T_{oo}, °K	293	293	293	293
T_{05}, °K	508.2	513.6	497.6	499.1
TR	1.735	1.753	1.704	1.709
% Increase in TR	Base	+1.0%	Base	+0.3%
$\Delta\eta_{TS}$	Base	+1.3 Point	Base	+1.0 Point

Table I above shows one trial to study coupling effects with CFD from 1997. Using a third party code, calculations were made with the impeller and vaneless diffuser and compared to tests with a vaneless diffuser downstream (a "so-called" uncoupled case). Then, more calculations were made with a coupled channel diffuser for the pr = 4.5 stage. The CFD showed a 4.6% impeller pressure increase for the coupled case vs. data showing 2.4% (about 2x error) and 1% increase in the total temperature rise vs. a measured 0.3% increase, or about a 3x error. The fact that these tended to wash out a bit for efficiency, so that CFD showed a 1.3% gain and data showed a 1% gain, is largely beside the point, as both pressure rise and power consumed are really the true metrics of a good product, and these were missed. Hence, it was realized in 1997 that much had to be done to capture the true flow physics.

2.4 General Overview, Phases I - V

CFD was used for general design guidance for all the work done in the 1990s, but it has come a lot further in the years since. Later sections will show that this tool has become vital to in-depth study of some of the key phenomena of these projects.

3.0 NEW DATA AND OBSERVATIONS

3.1 Vaneless Comparisons, Old and New, with Traverse Results

All data for the Phase VI consortium were taken with the test rig shown in Figure 20 below. This is a very precise rig, where every dimension is known to about +- 0.001 or 0.002 inch. The measurement error levels are very low, and repeatability is generally very good. Experimental methods meet or exceed ASME PTC 10 standards.

This rig has two different inlet ducts; the short one is now used for all basic tests, except when traversing is needed, in which case the long inlet duct (original 1990s) is used to get sufficient working space. The rig has been validated with two different upstream plenum arrangements and two different downstream orifice and throttle arrangements; no impact on performance has been observed. The rig was also evaluated with several different screens in front of the stage, and no effect was found. The rig is thoroughly insulated, and hence, it is adiabatic. It is operated with a turbine inlet temperature that is closely matched to the compressor discharge temperature so as to eliminate heat transfer through the bearing housing.

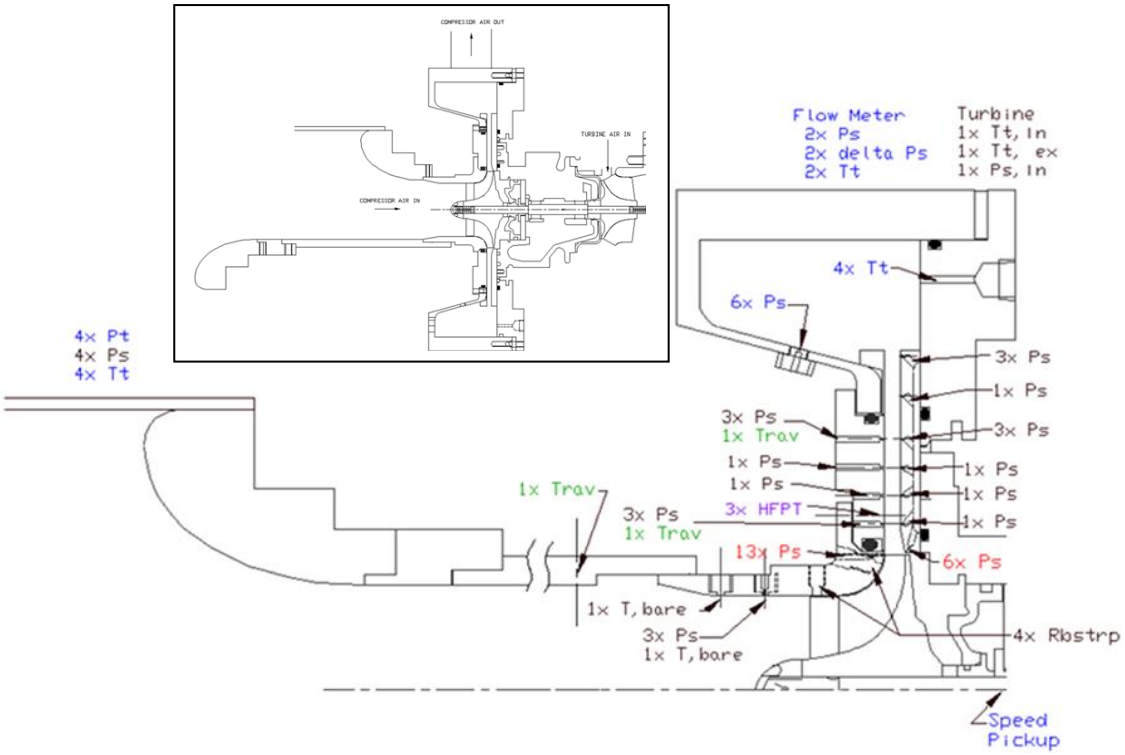

Figure 20. The 60 mm rig as used for Phase VI investigations with a rear pinch vaneless diffuser, the machined 16-bladed turbocharger impeller, and a long or short inlet duct The long inlet duct (see bottom of inset) is necessary to gain access for traversing.

Throughout the Phase VI work, great attention has been given to the vaneless modes of operation, as it was expected that this approach would lead to insights concerning rotor-stator coupling. This work began by selecting key cases from the 1990s investigations, and then repeating them with much greater instrumentation and flow visualization. The 25% front and rear pinch cases plus the 50% balanced pinch cases were thus tested in detail. In most cases, the original hardware was reused, with essentially no changes from the 1990s except that the operating clearance was set at 0.009 inch including the inlet eye clearance, which had been much larger on the Phase I work and some of the early Phase II work.

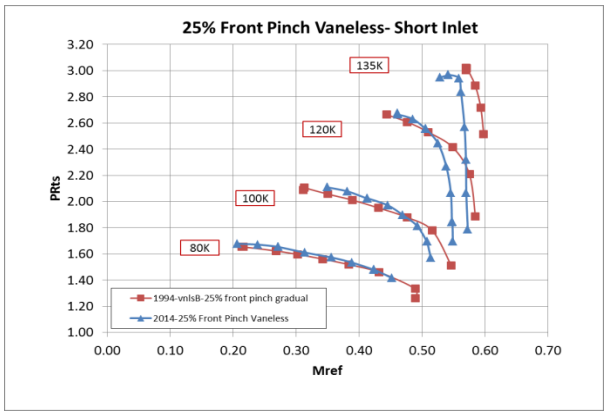

Figure 21. Pressure ratio for 25% front pinch for 1990s (red) and 2014 (blue) Inducer choke at high speed reduced due to tighter eye clearances after Phase I.

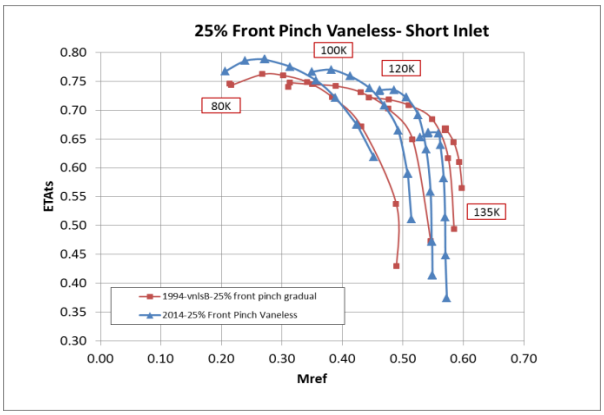

Figure 22. Efficiency for 25% front pinch for 1990s (red) and 2014 (blue)

The shift in high-speed choke (Figures 21 and 22) is due to larger eye clearances in the 1990s work. Current tests show slightly greater efficiency, perhaps due to better clearance control and better impeller surface finish, etc.

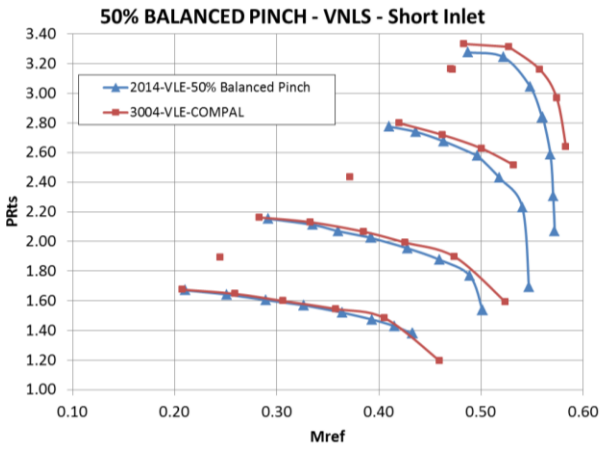

Figure 23. Pressure ratio for 50% balanced pinch for 1990s (red) and 2014 (blue)

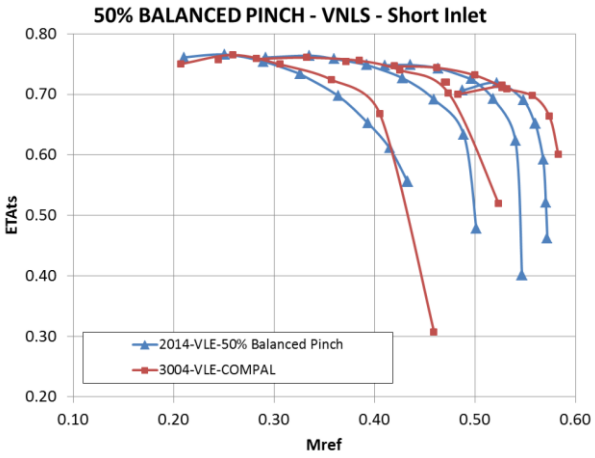

Figure 24. Efficiency for 50% balanced pinch for 1990s (red) and 2014 (blue)

The shift in high-speed choke is due to larger eye clearances in the 1990s work. The 50% pinch case, above, shows the same efficiencies.

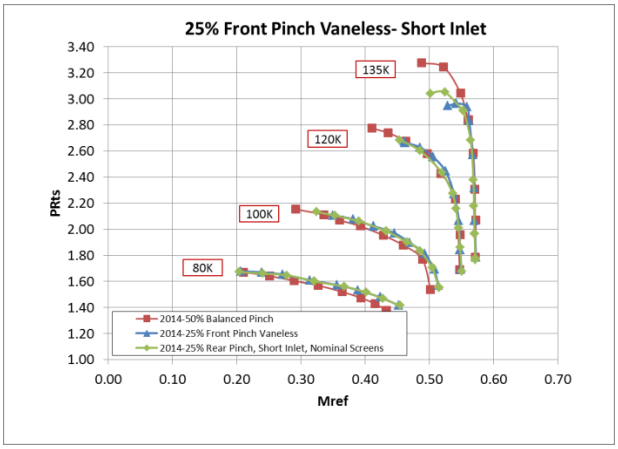

Figure 25. Pressure ratio for various pinch schedules

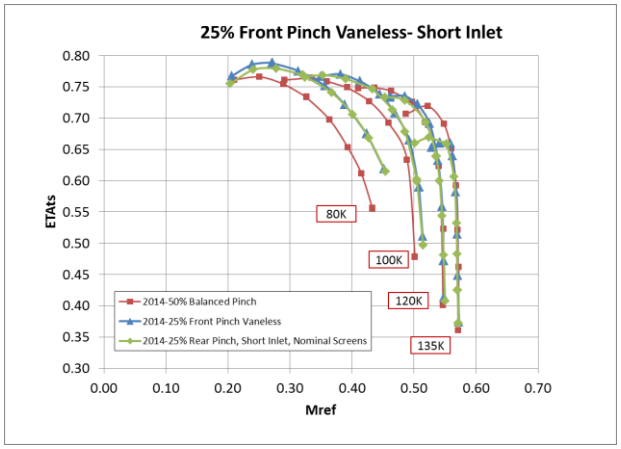

Figure 26. Efficiency for various pinch schedules

The balanced and rear pinch clearly outperform front pinch. Pinch strongly affects conditions along the surge line, as well as efficiency.

The detailed data obtained for the new tests afford many opportunities for further study. For example, the sample traverse data in the diffuser permit careful testing of the CFD codes, as shown later. A representative set is shown below in Figure 27.

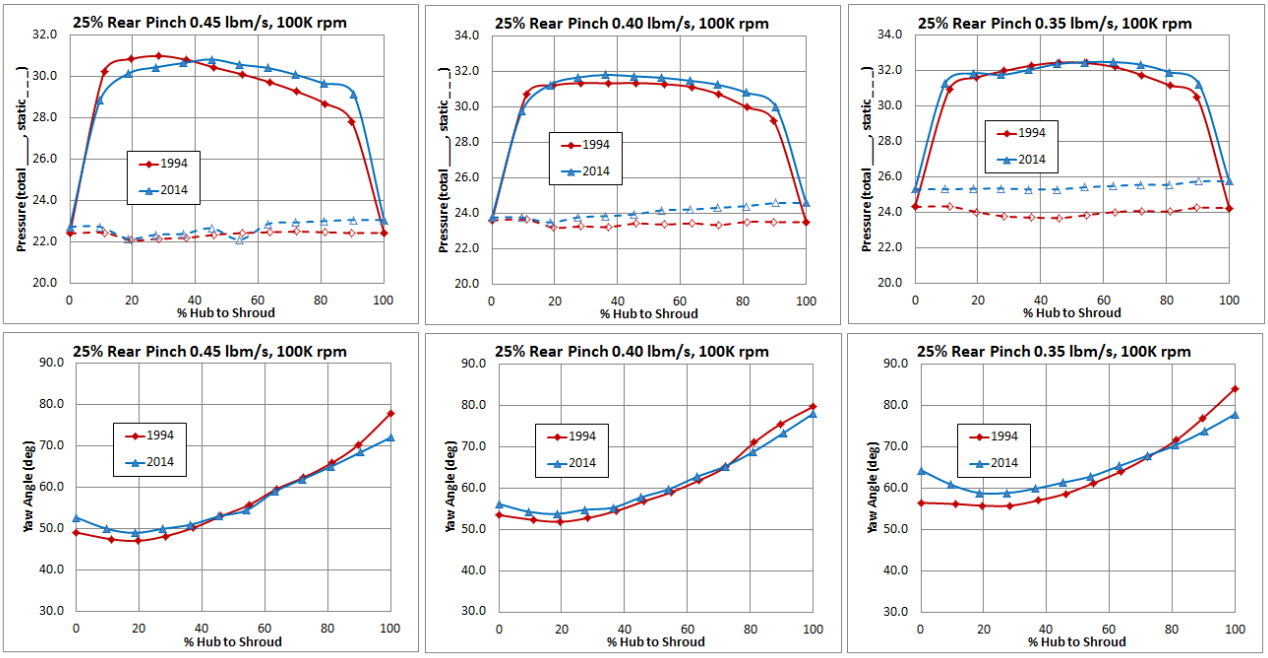

Figure 27. Comparisons of traverse data from the 1990s and 2014

Notice the last flow angle on the right-hand side of each plot above. For the 2014 data, the value is always lower, and this has contributed to better flow stability along the surge line; this may have been the result of a small design change in the impeller exit blading. The recent testing is far more comprehensive than the limited data of the 1990s. Figure 28, below, shows the static pressure change along the two diffuser surfaces; for the case shown, a 55% pressure gradient is measured across the impeller exit (55% of the p_2 value). More details are available in Appendix 5.

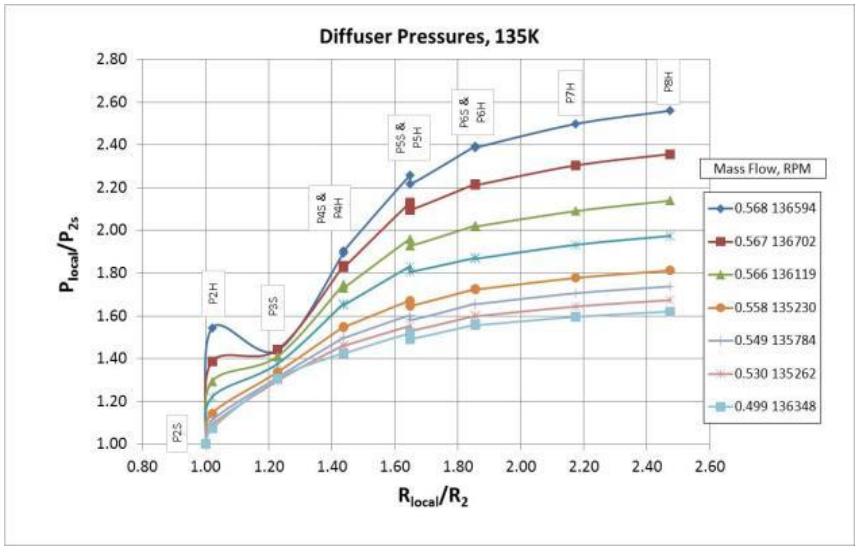

Figure 28. Static pressure rise along each side of a vaneless diffuser
The pressures are nearly the same on each side except near the inlet, where gradients may be found across the impeller exit/diffuser inlet of 55% of the impeller static pressure rise.

3.2 Vaned Comparisons, Old and New

Retesting of the selected vaned diffusers confirmed the original results, but added much needed internal data as well. Both the LSA and flat-plate diffusers and the lessons thereof from the 1990s have been confirmed. The details will be vital for subsequent CFD validation checks.

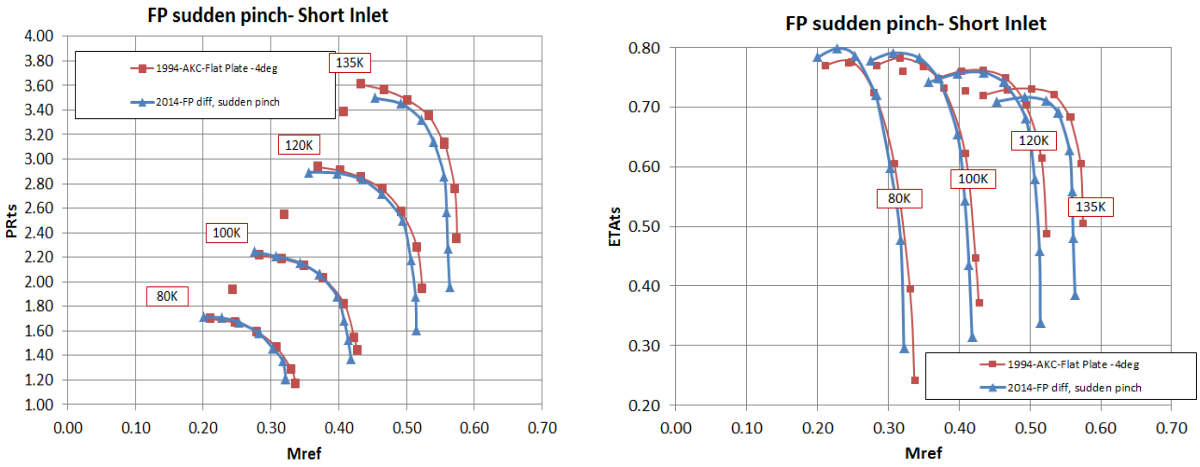

Figure 29. Flat-plate diffuser performance showing some improved efficiency and similar performance to 1990s results

3.2.1 Radial Pressure Variations

Radial pressure measurements through the various cascade diffusers, at each speed line and with each flow rate, have been recorded and will be valuable for CFD comparisons. An example is shown at 120,000 rpm in Figure 30. The variation with flow rate is normal and to be expected. The rise in pressure is very healthy, and no large scale defects are evident at all. It is worth noting the final variation in static pressure, where the penultimate measurement is made back in the diffuser at about 85% diffuser length, and the final measurement is made in the collector. Small changes are to be noted, the largest being at high flow rates. More details are available in Appendix 6.

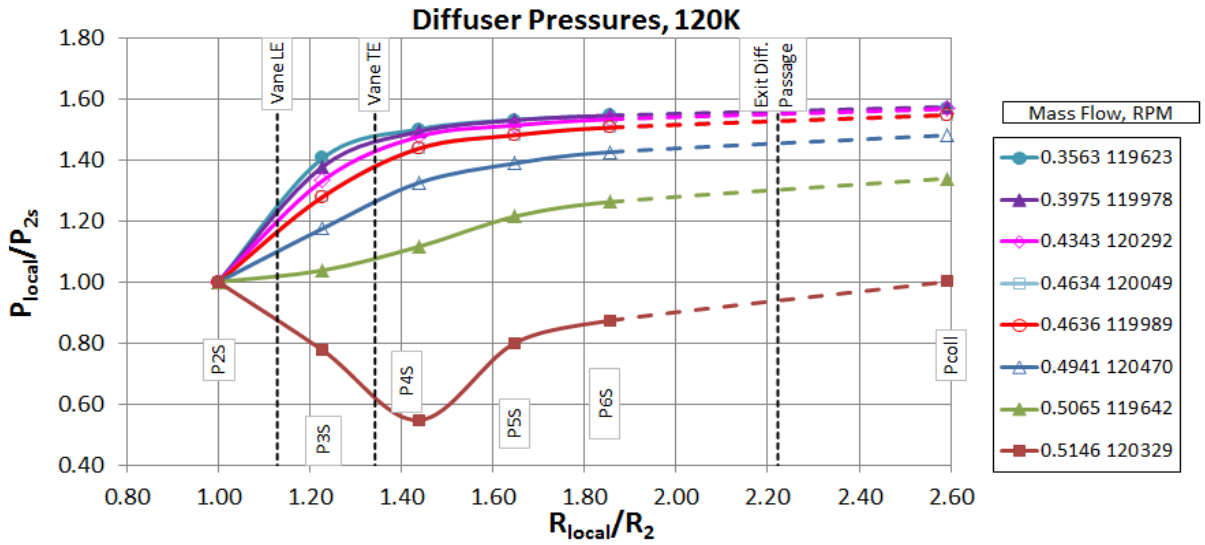

Figure 30. Radial pressure variations through a cascade (LSA) diffuser for the 120,000 rpm operating line

3.2.2 Circumferential Pressure Variations

Circumferential pressure variations were found in all builds, with some of them being quite small and others of noticeable magnitudes. The collector showed only the faintest of pressure variation (+-0.2 psia), which is truly negligible; it is a classic distortion that increases in magnitude as the flow rate increases.

The vaneless diffusers also showed some distortion at the impeller exit/diffuser inlet, and it was as much as +-0.4 (see Figure 31). While these distortions are real and of basic fluid dynamic concern, they are probably small enough that they can be ignored for basic CFD flow analysis (assume periodic boundary conditions). They are often strongest at low flow rates.

The vaned diffuser distortions are of considerable note. They have magnitudes up to +-1.5 psi and are not periodic at all, as shown in Figure 32. The diffuser distortions are not caused by the collector, and they do not vary with flow rate in the classic sense at all; the distortions can be large at either low or high flow rates.

Details of the distortion studies are given in the full report. A total of at least five different rigs have been identified, two of them from these historical studies, where this characteristic has been observed (see Appendix 7 for details).

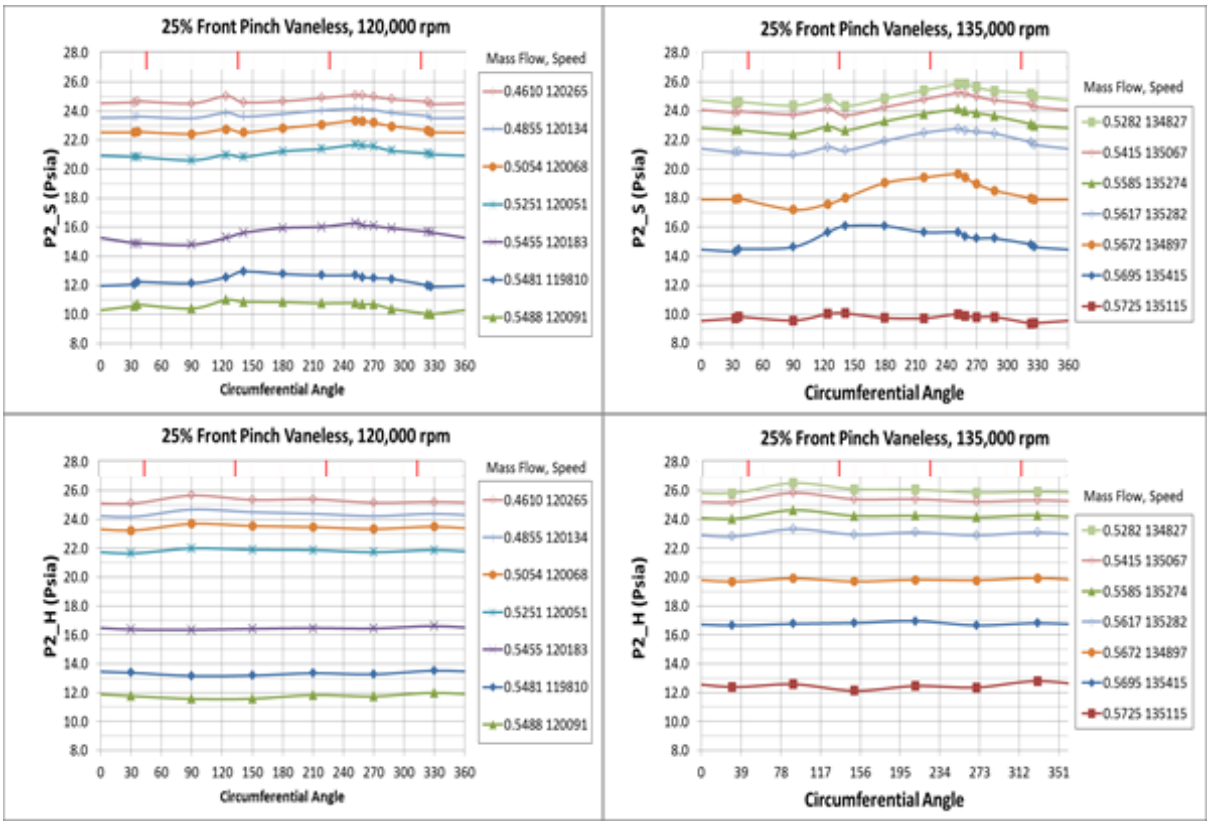

Figure 31. Circumferential pressure variations for a vaneless diffuser test set; the distortions are **NOT** traceable to any rig geometry and are thought to be a natural flow phenomenon

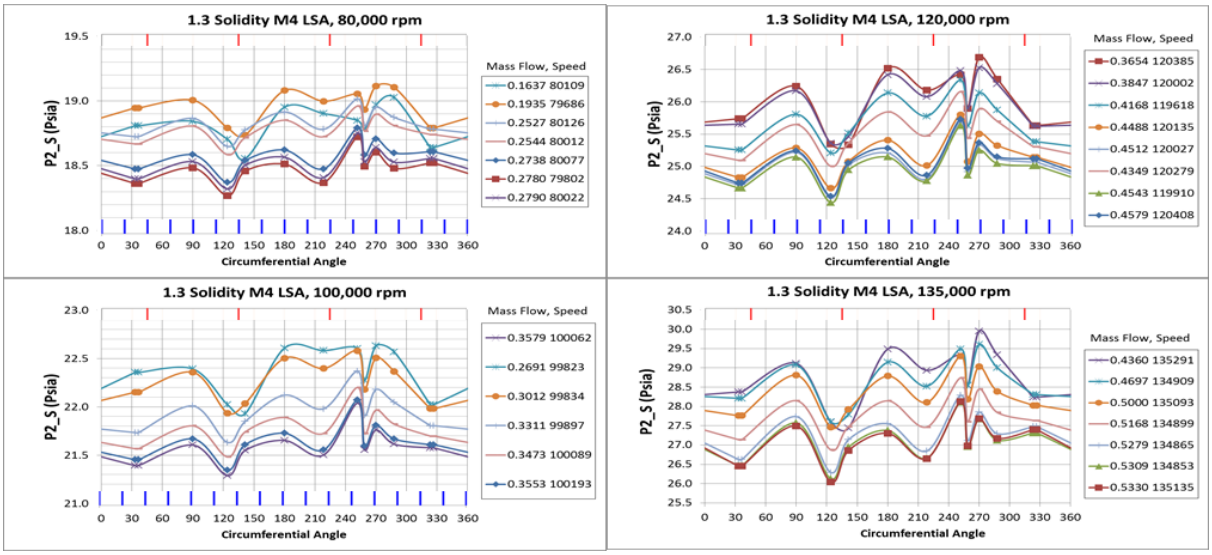

Figure 32. Circumferential pressure variations for a vaned diffuser test set; the distortions are **NOT** traceable to any rig geometry and are thought to be a natural flow phenomenon

Understanding these distortions may be important for unraveling the mysteries of impeller and diffuser coupling. Just recognizing their existence is a very important step towards an eventual solution to the coupling problem.

3.2.3 Grooved Covers

The studies in Figures 31 and 32 show strong evidence of asymmetric flow. Later, flow-wise cover grooves are introduced to improve the flow field in general; it remains to be seen, but it is possible that these grooves may reduce these erratic pressure variations.

3.2.4 Other Observations

High-frequency pressure measurements have been made at various points in the operating flow field. No rotating stall has been found. Also, flow visualization has been conducted at many points near the surge line for various configurations and at various locations in the test stage. No backflow has been found at any point in the flow field except the cover leakage flow, which is always in backflow but does NOT enter into the inlet pipe. The use of thermocouples in the inlet to look for backflow has been discredited (see Appendix 7 for details).

4.0 MODERN LESSONS FROM CFD

4.1 Basic Flow States

Detailed CFD studies were made, and comparisons carried out for the front, rear, and balanced pinch cases at each of the eleven (11) flow traverse points using the 1990s data. One case is shown here, and for this one, the data were taken at 80,000 rpm and a mass flow of 0.306 lbm/s, while the CFD simulation is at a mass flow rate of 0.280 lbm/s. The rest of the cases may be found in Appendices 4 and 5. Numerous comparisons such as in Figure 33 give reasonable confidence in the CFD modeling now possible.

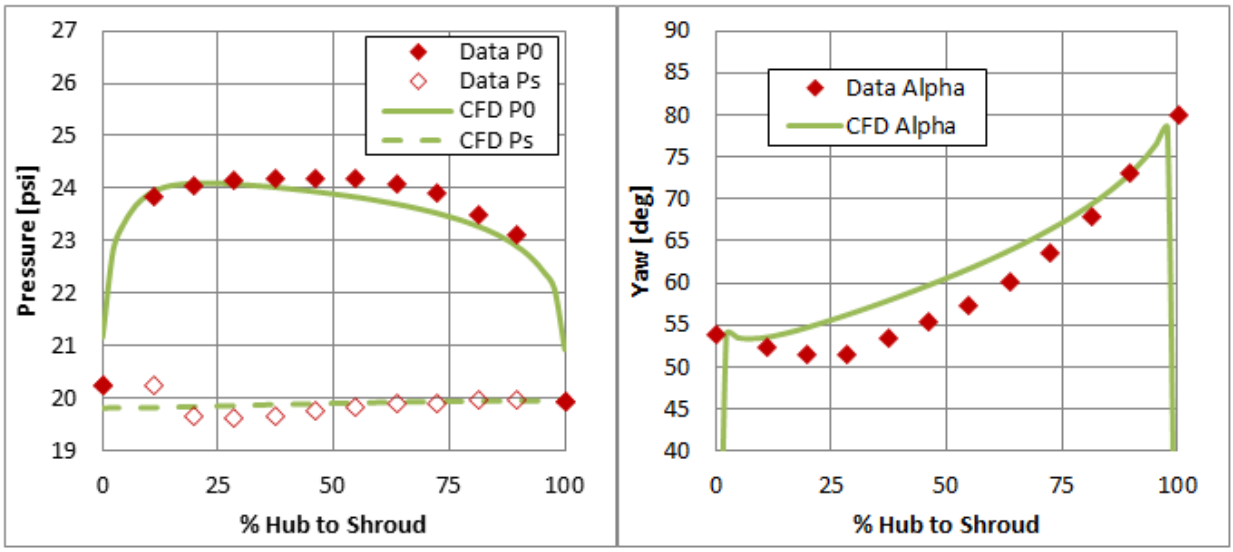

Figure 33. Traverse data CFD comparison for 25% vaneless hub pinch geometry

Figures 34 – 37 show the absolute flow angle, efficiency contours, meridional velocity, and tangential velocity at various meridional positions, both before and after the impeller trailing edge. This point is located near the surge line. It does show shroud side meridional velocities approaching zero, but the absolute flow angles do not hit 90°. In each diagram below, there are a series of passage cross sections, starting at 70% impeller meridional distance and going out to 130%, i.e., into the vaneless diffuser. On the bottom cross section, there are two reference lines labeled M1 and M2. These locate and refer to the two meridional cuts that are displayed on the right side of each figure.

Figure 38 displays several comparisons of the computed flow leaving the impeller for each type of diffuser pinch. It is very clear that the work input and the pressure rise for the impeller is changing significantly, depending on the type of pinch used in the diffuser. Contours of meridional velocity, efficiency, and flow angle confirm the same story. More information on these studies may be found in Appendix 4.

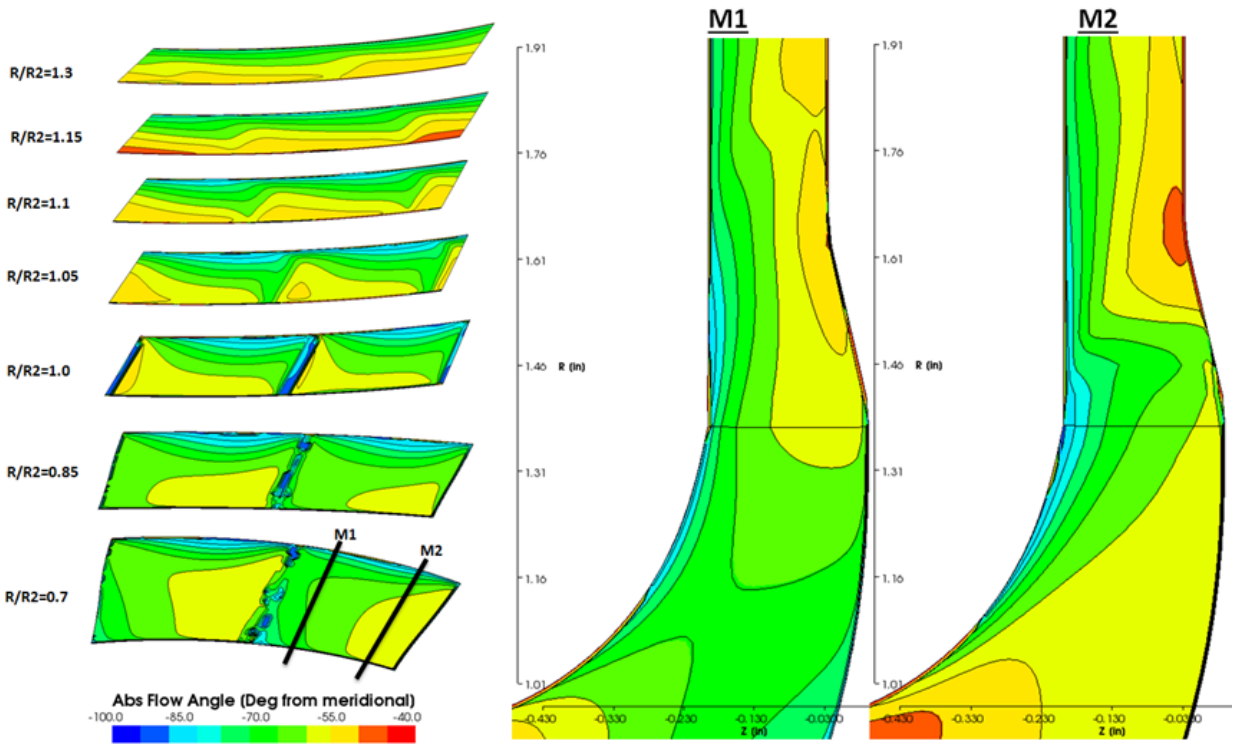

Figure 34. Absolute flow angle contours from CFD simulation results for 25% vaneless hub pinch geometry at 80,000 rpm and a mass flow of 0.280 lbm/s

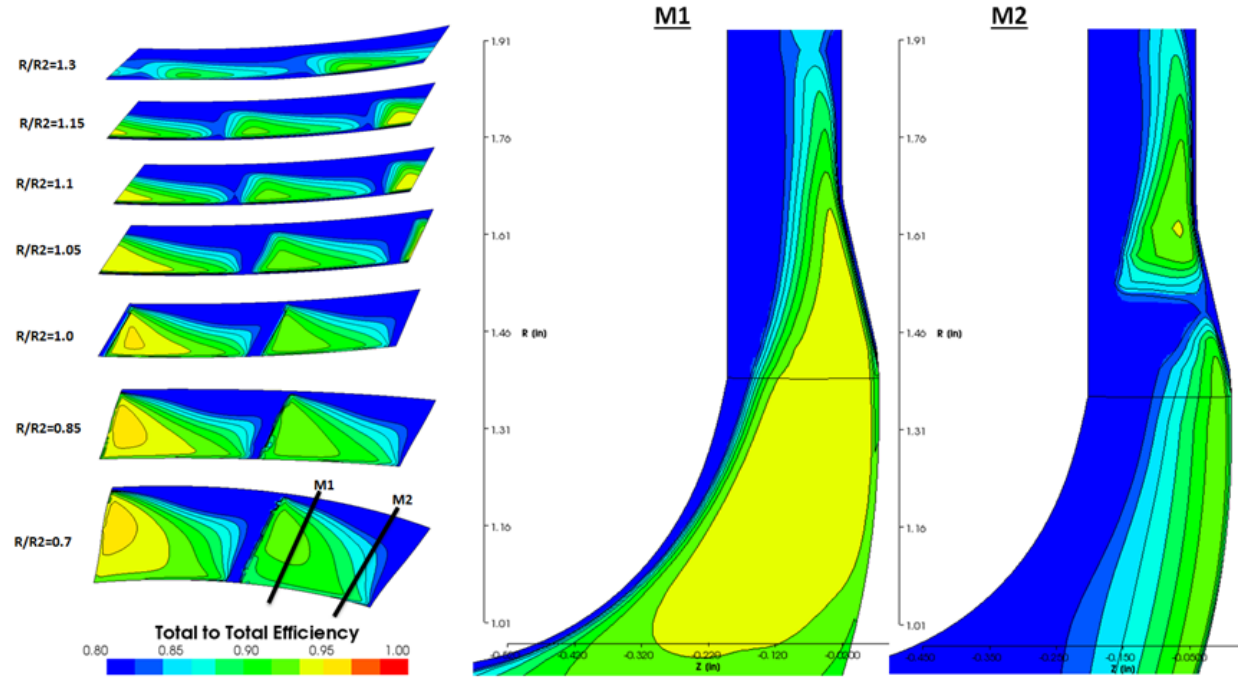

Figure 35. Contours of total-to-total efficiency from CFD simulation results for 25% vaneless hub pinch geometry at 80,000 rpm and a mass flow of 0.280 lbm/s

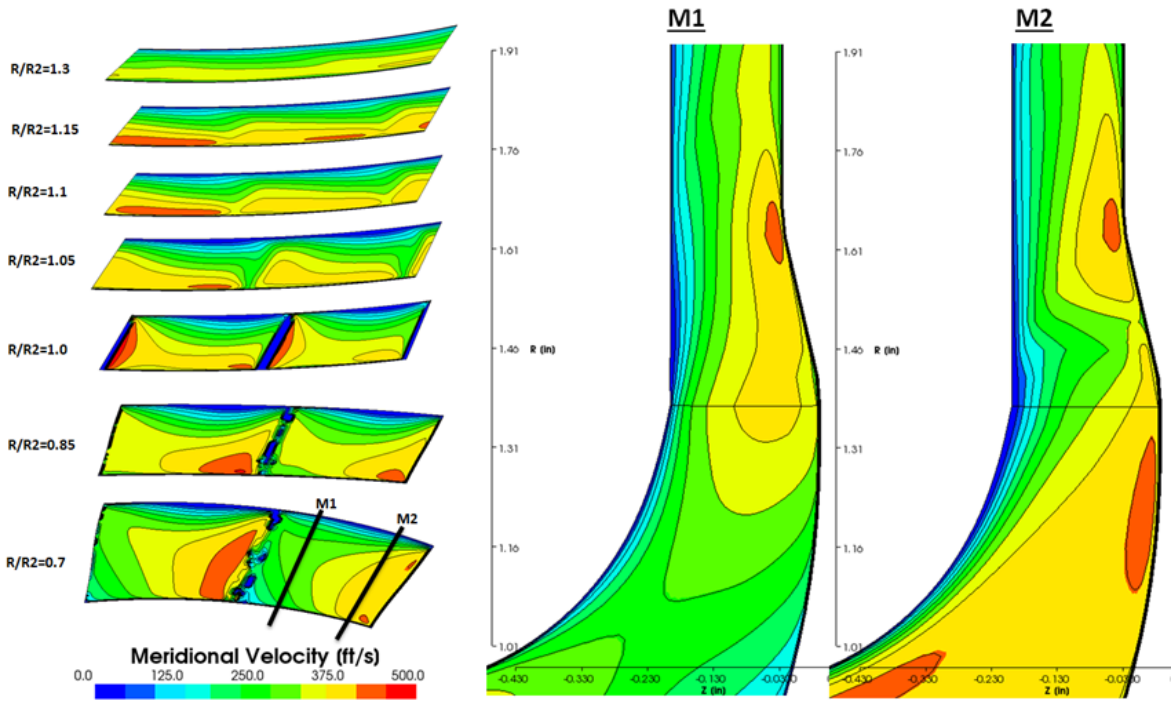

Figure 36. Meridional velocity contours from CFD simulation results for 25% vaneless hub pinch geometry at 80,000 rpm and a mass flow of 0.280 lbm/s

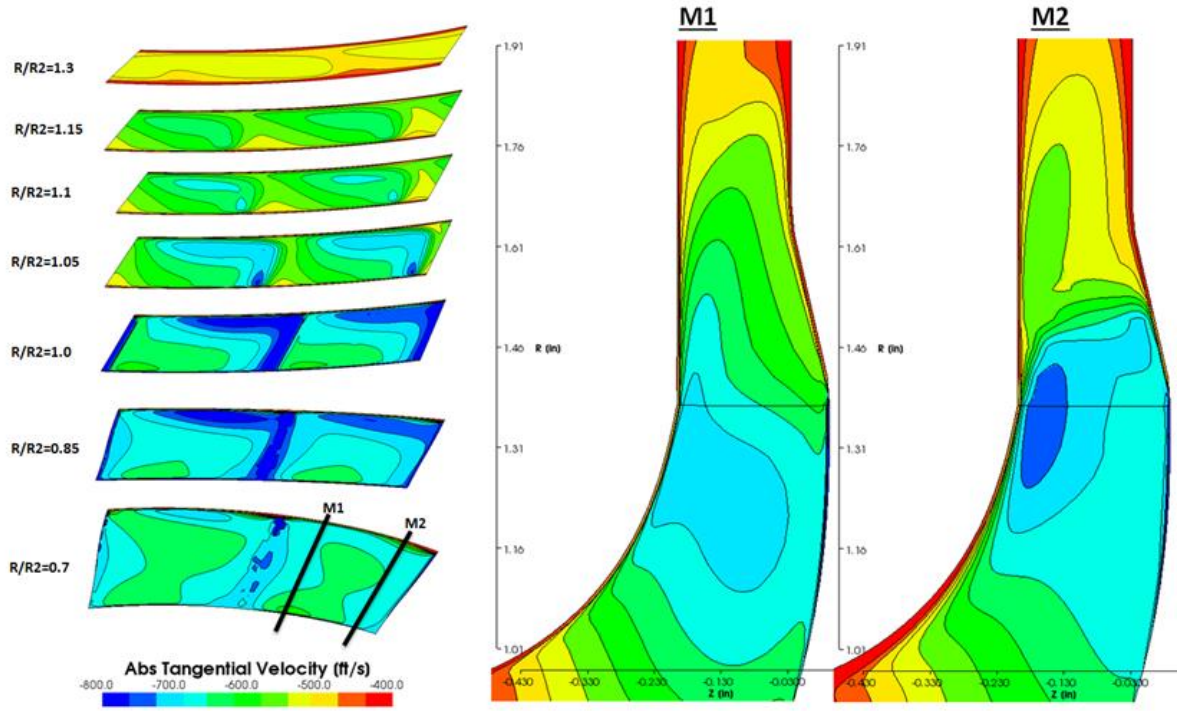

Figure 37. Tangential velocity contours from CFD simulation results for 25% vaneless hub pinch geometry at 80,000 rpm and a mass flow of 0.280 lbm/s
Please ignore the negative sign on the legend – it is a known glitch; they are positive!

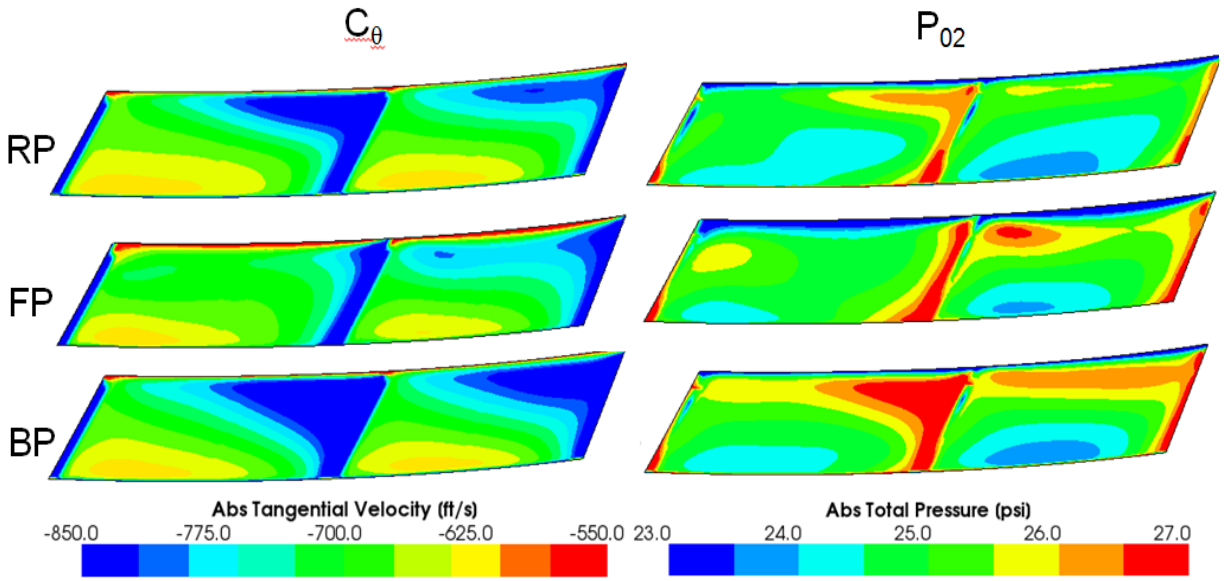

Figure 38. Comparisons of impeller exit states for rear pinch (RP), front pinch (FP), and balanced pinch (BP) showing changes in impeller exit flow state depending on pinch type This point is taken on the 80,000 rpm line near surge. See Appendix 9 for more details.

4.2 Validation (CFD Mini-Olympics)

In order to have a strong validation process, *CN* has established an ad hoc CFD Mini-Olympics to test various codes and approaches. Presently, two major codes are in use, including Pushbutton CFD®[1] (PbCFD) and Solver A. All exterior codes will be identified on a blind basis.

For the first test case, only the in-house code has been used so far; Solver A results will be added later. Figures 39 and 40 show excellent agreement between the CFD and data for the front pinch case.

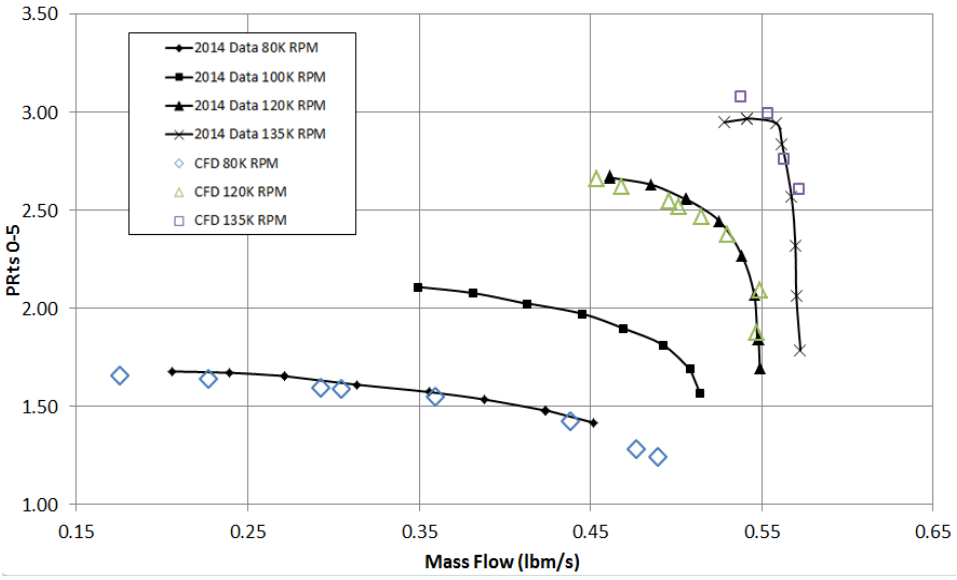

Figure 39. Front pinch vaneless diffuser; CFD Mini-Olympics (next candidate) showing PbCFD and current data; good pressure rise agreement at all speeds; Solver A to be added

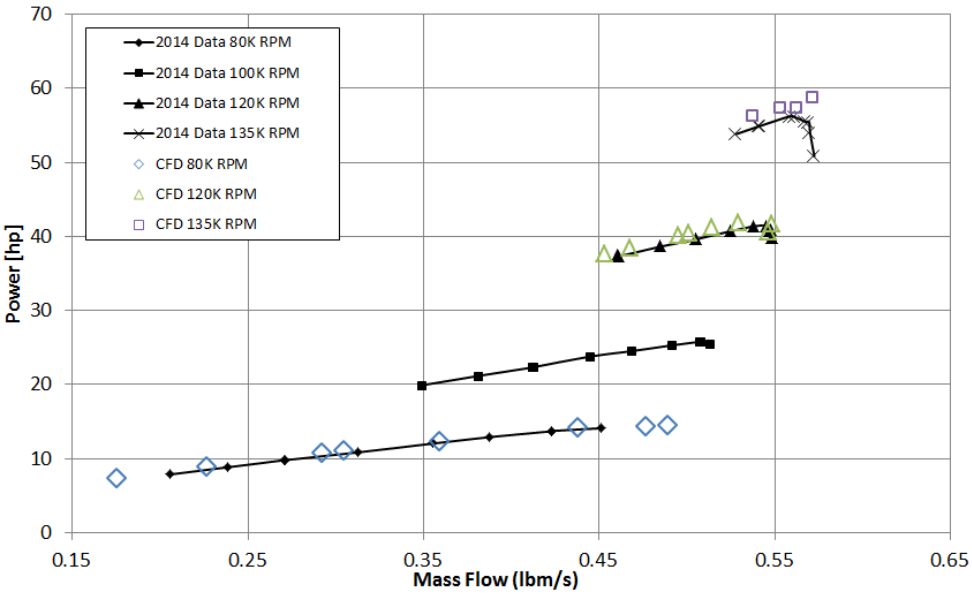

Figure 40. Front pinch vaneless diffuser; CFD Mini-Olympics (next candidate) showing PbCFD and current data; good power agreement at all speeds; Solver A to be added

[1] Pushbutton CFD is a registered trademark of Concepts NREC, LLC.

The results shown below for the rear pinch case are interesting, with more details included in Appendix 9. Excellent agreement on pressure (Figure 41) and power (Figure 42) has been achieved on the 80,000 rpm line. For the 120,000 rpm and the 135,000 rpm lines, there is a definite offset on pressures and an over-prediction on power with each code. This situation is under review and does have noticeable variations at other pinch conditions. Both Figures 39 and 41 show the same inducer choke levels for the data, but not the CFD. Distortion may be part of the explanation here; more discussion is found in Appendix 9.

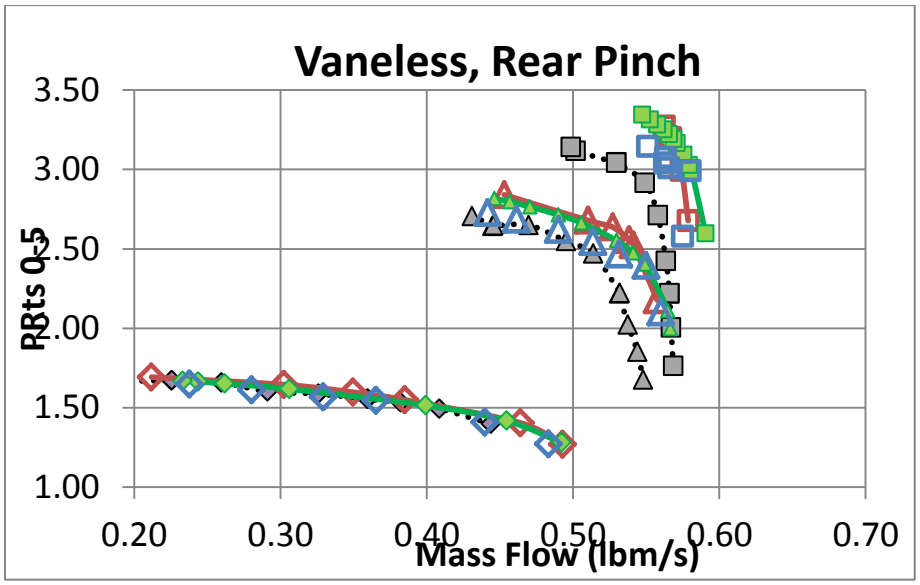

Figure 41. Rear pinch vaneless diffuser; two major codes and current data - good agreement at 80,000 rpm, fair agreement at higher speeds
Old CFD was run with a coarser model for leakage and seems closer to nature

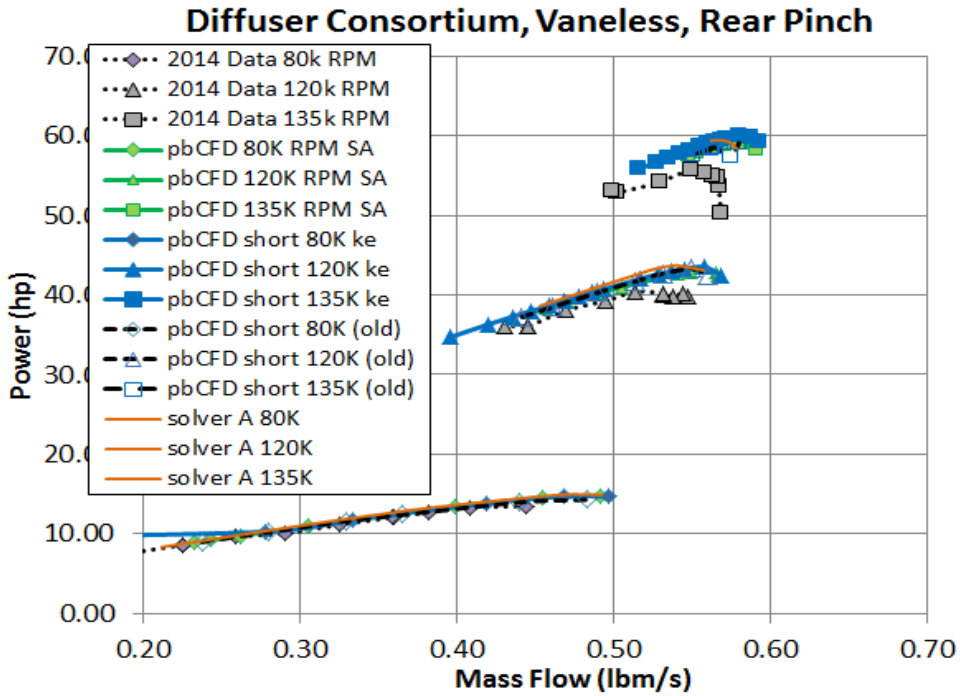

Figure 42. Rear pinch case with good agreement on power at low speed, close at 120,000 rpm and off a bit at 135,000 rpm; contrast these results with the front pinch case above

Cases with vaned diffusers will be added shortly.

Studies with the CFD calculations have been diverse and useful. Turbulence models have been checked, and with appropriate corrections, no differences in overall predictions using either the Spalart-Allmaras or the k-ε modules have been found.

Inlet studies are also underway at this time. Unusual inlet enthalpy effects have been found that are receiving special attention. Also, study of the clearance modeling is underway.

4.3 Pinch Study

Some attention has been placed on the question of diffuser pinch, and with some reasonable success. The effort also gave a good chance to judge the voracity of current day CFD calculations. Pinch was found to be very important in the 1990s study in Phases I – V. It is very difficult to model, and earlier attempts failed to establish a credible base for understanding and for design.

In the graphs below, the 25% front and rear pinch vaneless diffuser CFD and measured data (1990s) are displayed for comparison. The first figures, 43a & b, give a comparison of the directly measured and computed stage pressure ratios. Figure 43a shows the modeled CFD calculations, and Figure 43b shows the measured data. There is close similarity between the data and CFD trends, except that the 120,000 rpm lines are a bit more separated in the CFD than as shown for the measured data. The next two Figures, 44a & b, compare efficiencies for CFD and data, respectively. The trends are again quite similar between computation and data, with the correct separation between cases for the 80,000 and the 135,000 rpm sets. For the 120,000 rpm case, the separation is a bit exaggerated in the high flow end. This is also the same for the work input coefficient, as shown in Figures 45a & b.

Overall, these characteristics are well modeled by PbCFD, and the difference between the two pinch cases is moderately well distinguished. Nonetheless, when the detailed traverse data sets are reviewed, the comparison is not as good for the front pinched case. Effects of natural flow field distortions and complex blade shroud leakage flows are still of concern for rigorous modeling.

There is reason for some optimism that pinch effects at the inlet of vaneless diffusers can be modeled. It should be stressed, however, that this will not necessarily translate to vaned diffusers. These calculations have all been conducted in the relative frame of reference, and hence, no mixing plane or other contrived boundary state has been imposed between the impeller and the diffuser. Unfortunately, it is not possible to take this approach for vaned diffusers.

A related study is shown in Figure 44 where the front and rear p_2 measurements are compared with CFD modeling. It may be observed that this important detail is quite well modeled, and perhaps with some more grid refinement, even better agreement may be found. These calculations are compared with the average value of the pressures, hence averaging out the distortions discussed above.

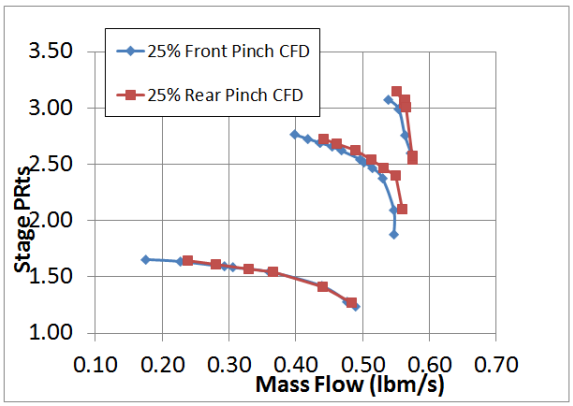

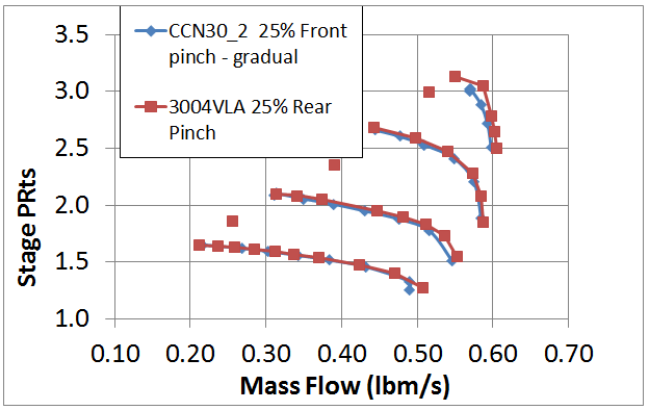

Figures 43a & b. 25% pinch vaneless diffuser stage performance maps
a) CFD on left, and b) test results on right

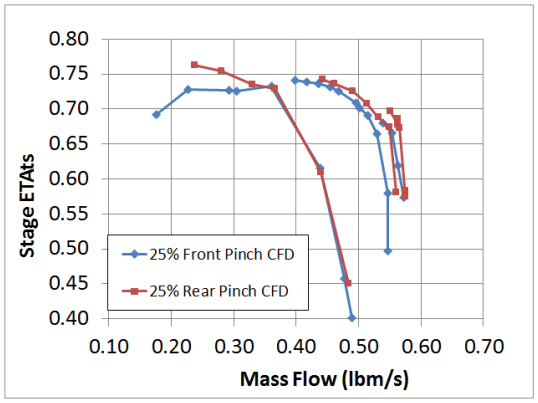

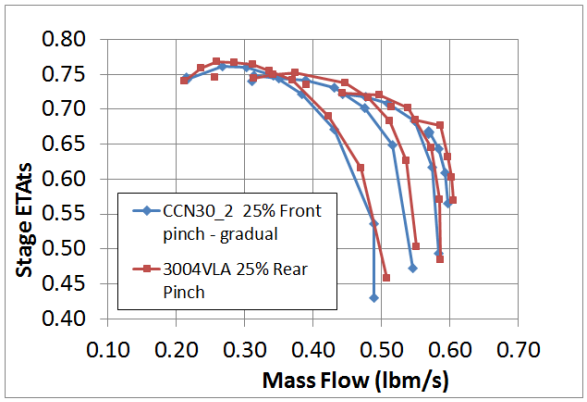

Figures 44a & b. 25% pinch vaneless diffuser stage efficiency maps
a) CFD on left, and b) test results on right

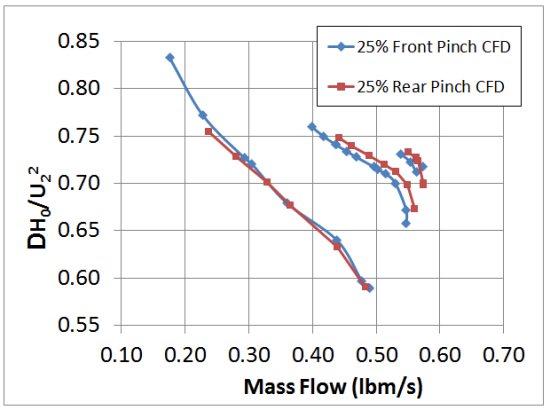

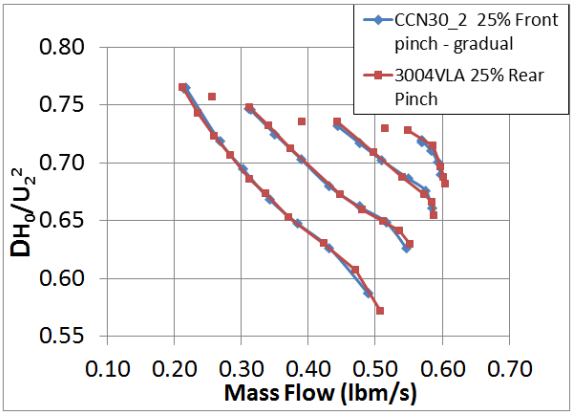

Figures 45a & b. A comparison of CFD and data for the work input coefficient
a) CFD on left, and b) test results on right

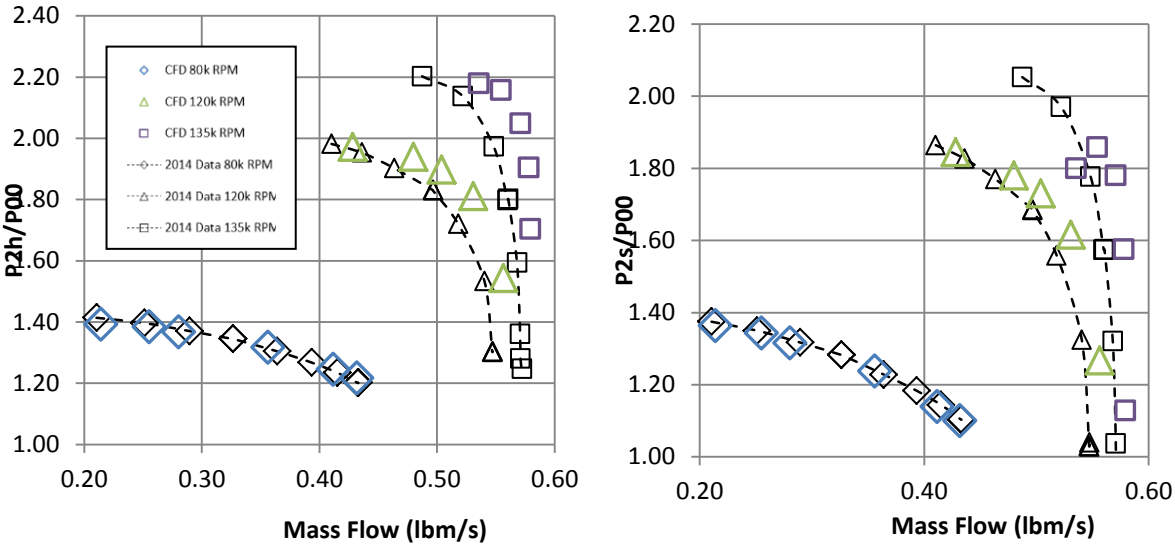

Figure 46. A comparison of measured p_2 (impeller exit) pressures on the rear and front cover and at various speeds and flow rates with the CFD analysis Generally, good predictions have been achieved.

4.4 Grooved Cover Results

The grooved cover was inspired by recognizing that the passage secondary flow was frequently located near one of the bounding surfaces, and frequently, it was the front shroud surface. This secondary flow gives large passage blockage and very bad flow angle variations between the core flow and the secondary flow; by using some of the secondary flow and realigning it in the absolute frame of reference to a better exit angle, it should be possible to improve stage performance, as is covered in US Patent 8926276B2. Figures 47 and 48 each show one embodiment of the concept. Figures 49 and 50 illustrate some of the gains achieved by this novel method. Further examples and details are to be found in Appendix 8.

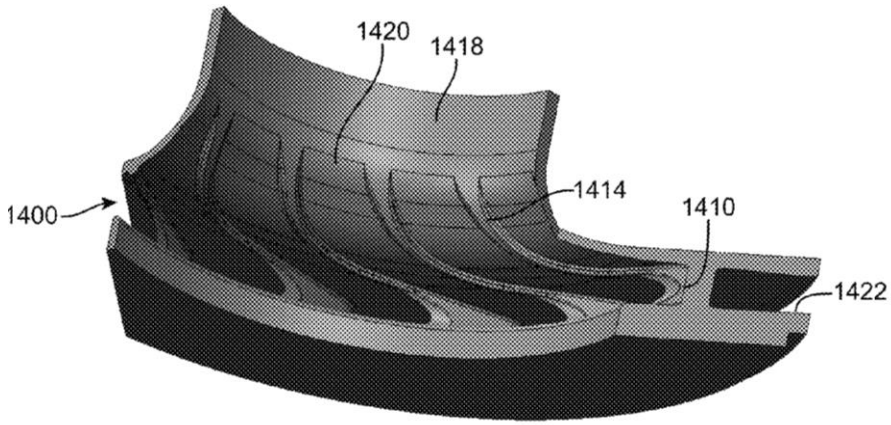

Figure 47. An embodiment of the flow-wise grooved cover treatment (US Patent 8926276B2)

Figure 48. Hardware for another embodiment of the flow-wise grooved cover

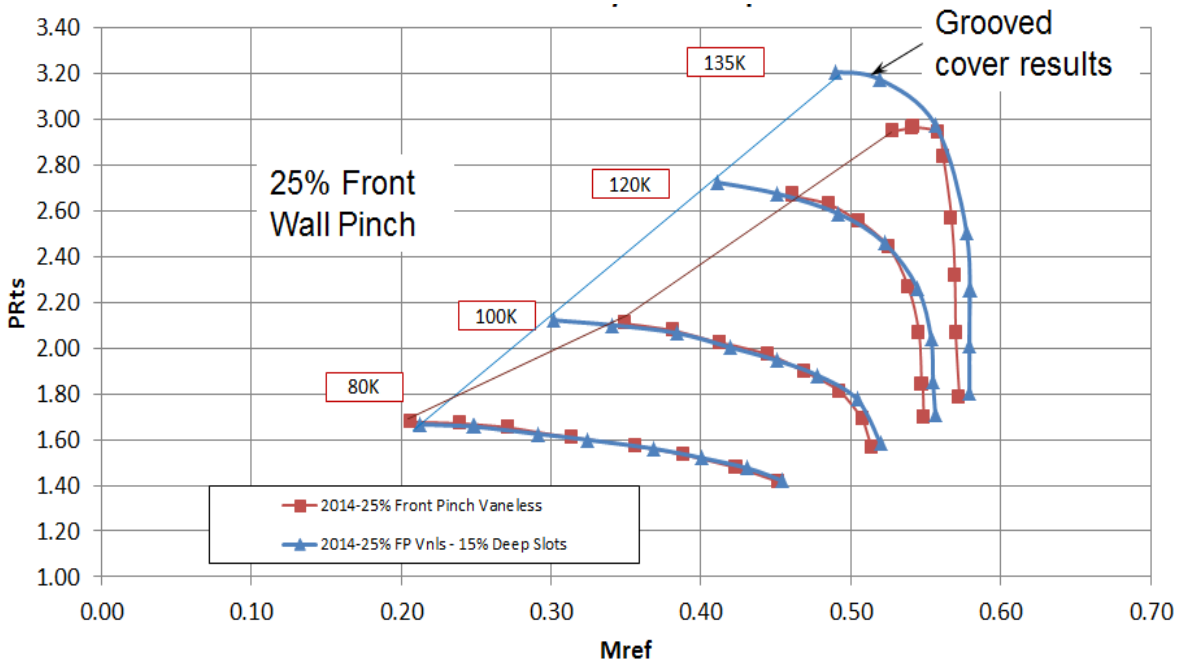

Figure 49. Test results for the Figure 48 embodiment of a flow-wise grooved cover Efficiency has been improved in a key part of the map, range has been extended, and a much healthier surge line has been achieved.

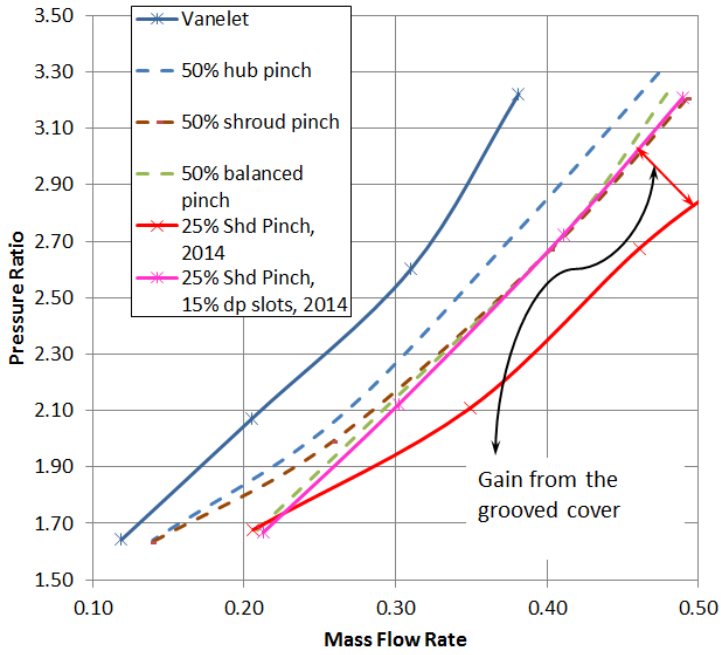

Figure 50. Improved surge line brings the 25% shroud pinch case up to the 50% shroud pinch case without suffering the same degree of losses

4.5 CFD Observations

Preliminary methodology to guide the design of the grooved covers has been based on CFD; this work is described in Appendix 8.

4.6 Fundamental Questions

Throughout this project, we have listed and discussed the key conceptual questions which need answers so as to design advanced diffusers with confidence. The historical list is:

1. How do diffusers and impellers couple together, and how does this coupling change performance of the stage?
2. How does diffuser pinch change performance of a diffuser, and why is front and rear pinch so different in certain cases?
3. Is there a strong gradient in static pressure at Station 2 caused by this pinch?
4. Why did early CFD studies fail to model the effects of pinch?
5. Why did the small flat plate diffuser emerge as one of the best diffusers of the 1990s consortium studies? Why did it fail in in certain limited other cases?
6. How can these coupled flow fields be modeled in meanline codes? How can accurate C_p values be calculated? Is there recirculation involved in these impellers?
7. How can these coupled flow fields be modeled in CFD codes?
8. What is the best design envelope of LSA diffusers?
9. When is a channel diffuser the best choice?
10. When is a conical diffuser the best choice?
11. Are there other shapes of diffusers that are superior?
12. Why is the continuous crossover such a good performing diffuser?
13. How compact can a diffusing system be made?
14. What is the best volute to be used with each class of diffuser?
15. Why can two classes of diffusers have nearly the same performance, yet have vane counts that are 2 or 3 times different with much different wetted areas?
16. How much impact can these questions have on diverse commercial products today?
17. Can C_p exceed 80% for any class of diffuser?

To this list we must now add the following:

18. What is the proper modeling of the clearance gap flow?
19. Why do circumferential distortions in static pressure exist; can they be controlled?
20. Why are there gradients in total temperature computed in front of the impeller?
21. How do we model the grooved cover, which are two computational frames coupled dynamically?

Progress has been made on answering these questions; several of them can now be considered fully answered, whereas others need more probing before we can be confident of solid answers. Detailed discussions of these points can be found in Appendix 10.

5.0 SUGGESTED NEXT STEPS

1 A number of sponsors and potential sponsors have asked for a broader study base. Work in Phases IV and V established such a base with three different impellers and a wide variety of vaneless, LSA/flat, channel/conical diffusers. With these, it is now possible to:

- Continue High Ns (110) stage (pr = 3.5) for limited tests to complete matrix,
- Pursue pr = 4.5, Ns = 85 stage with a good set of diffusers, and
- Pursue pr = 1.8, Ns = 55 stage with vaneless, LSA, and flat-plate diffusers.

Possibilities for study include the options suggested in the following table:

TABLE II. DIFFUSER STUDY POSSIBILITIES

Impeller Type	Testing per Diffuser Class and Type (y - yes; n - no; n/a - not applicable)												Grooved Covers	
	Vnls-f	Vnls-r	Vnls-b	Vnls-pa	Ch-t	Ch-a	Ch-d	Con	LSA	HSA	Tnd	Flat	Vnls	Vaned
Ns = 110, pr = 3.5	y	y	y	n	y	n	y	n	y	n	y	y	y	planned
Ns = 85, pr = 4.5	y	n	n	n	y	n	n	y/n	y	n	n/a	n	n	n
Ns = 55, pr = 1.8	y	n	n	n	n/a	n/a	n/a	n/a	y	n/a	n/a	n	n	n

Vnls-f = front pinch Vaneless	Ch-t = tangential divergence	LSA	= Low Solidity Airfoil
Vnls-r = rear pinch Vaneless	Ch-a = axial divergence	HAS	= High Solidity Airfoil
Vnls-b = both sides pinched	Ch-d = double divergence	TND	= Tandem Airfoils
Vnls-pa = partial height vanes	Con = Circular cross section	FLAT	= Flat Plate LSA equivalent

Once selected, the goal would be to have fairly broad coverage of the best diffusers in each flow coefficient range, so that best practices across the board can be established with and without grooves or other cover treatments. The highlighted elements of the table may hold promise for future development.

2 Study detailed clearance and passage plus grooved flows at impeller exit and diffuser inlet with L2F (Laser-Two-Focus velocimetry) with a vaneless diffuser.

- Conduct L2F measurements for a stage on the largest consortium rig, ca. 125 mm D2
- Evaluate data and test modeling of the same with CFD

3 Study detailed clearance and passage plus grooved flow at impeller exit and diffuser inlet with L2F with a vaned diffuser.
   - Conduct L2F measurements for a stage on the largest consortium rig, ca. 125 mm D2
   - Evaluate data and test modeling of the same with CFD

4 Study the set of best diffusers, and postulate a hybrid with the best characteristics of several. Design and test. For the vaneless case, find the key limits on low flow operation, and move them lower, if possible.

5 The grooved cover has worked well; it should also be tested in conjunction with other range extension methods such as inlet tip treatment, cover bleed, damper plenums, etc.

6 Flow-wise grooved covers have shown promise. To continue this effort, we should prepare a best grooved cover (range and efficiency improvement) for two stages, and continue the study; these may be for the Ns = 55 and Ns = 85 stages and may involve rear side grooves, as well as front cover grooves.

7 Time-accurate CFD
   - Assess practicality of existing codes to correctly resolve clearance and grooved flow issues
   - Assess means of extending codes
   - Pursue rational extensions of existing codes to deal with two frames of reference

8 Add a symmetric or an overhung volute designed in part by MDO to give the best area and radius distributions and tongue shape; test in vaneless mode. Use laser sintering to produce volute.

9 Update two-elements-in-series (TEIS) models for impellers
   - Revise correlations and update design database
   - Explore impeller and diffuser coupling effect on TEIS parameters for enhanced modeling capabilities

10 Update TEIS models for diffusers
   - Study behavior in new test data and compare to existing correlations
   - Add test data to design database and validate models
   - Improve numerical modeling capabilities for wider range of stationary vaned diffusing elements

6.0 REPORTING

A detailed report of Phase VI work will be issued before June 15, 2015. This present report is the public version of the Final Report overview, which will have more detail added, plus latest tests and analysis, before issuing. Comprehensive reports on various issues and details will be attached as appendices, as noted below; they will not be publicly available.

7.0 CONCLUSIONS

Work on Phase VI diffuser investigations is nearly done. New insights to the basic physics have been achieved, namely: 1) the flow fields are not inherently axisymmetric (some lack practical levels of periodicity), 2) some work may be done or unusual thermal effects are caused by rotating flow fields in front of the impeller blading, 3) the work input for the stage can be modified by using flow-wise grooves on the cover, without any change to the impeller, and 4) the surge line can be moved with flow-wise grooved cover treatment. CFD has been generally confirmed for solving some of the design issues, but areas of disagreement have been identified for future study. Proposals to extend and broaden this work have been developed.

8.0 APPENDICES

1 Project Statement of Work or proposal

2 Phases I – V work done

3 Laboratory setup and lab validation tests

4 Early CFD studies

5 Vaneless diffuser test results, including detailed traversing

6 Vaned diffuser test results

7 Distortion studies and related literature and cases

8 Grooved cover tests and CFD basis for designs

9 Detailed list of questions, comments, and conclusions